



Search for supersymmetry in final states with disappearing tracks in proton-proton collisions at $\sqrt{s} = 13$ TeV

The CMS Collaboration*

Abstract

A search is presented for charged, long-lived supersymmetric particles in final states with one or more disappearing tracks. The search is based on data from proton-proton collisions at a center-of-mass energy of 13 TeV collected with the CMS detector at the CERN LHC between 2016 and 2018, corresponding to an integrated luminosity of 137 fb^{-1} . The search is performed over final states characterized by varying numbers of jets, b-tagged jets, electrons, and muons. The length of signal-candidate tracks in the plane perpendicular to the beam axis is used to characterize the lifetimes of wino- and higgsino-like charginos produced in the context of the minimal supersymmetric standard model. The dE/dx energy loss of signal-candidate tracks is used to increase the sensitivity to charginos with a large mass and thus a small Lorentz boost. The observed results are found to be statistically consistent with the background-only hypothesis. Limits on the pair production cross section of gluinos and squarks are presented in the framework of simplified models of supersymmetric particle production and decay, and for electroweakino production based on models of wino and higgsino dark matter. The limits presented are the most stringent to date for scenarios with light third-generation squarks and a wino- or higgsino-like dark matter candidate capable of explaining the observed dark matter relic density.

Published in Physical Review D as doi:10.1103/PhysRevD.109.072007.

1 Introduction

Supersymmetry (SUSY) [1–9], a well-motivated extension of the standard model (SM) of particle physics, addresses open questions of the SM such as dark matter (DM) [10, 11] and the fine tuning [12–14] of the electroweak sector. Studies from the ATLAS [15] and CMS [16] Collaborations at the CERN LHC have placed significant constraints on the minimal supersymmetric SM (MSSM), with no direct evidence as yet for the existence of SUSY particles. Nonetheless, important regions of the MSSM parameter space remain unexplored, such as regions with a nearly pure wino- or higgsino-like lightest supersymmetric particle (LSP) that are consistent with the observed DM relic density [17].

A DM candidate can arise in SUSY if the LSP is stable, as occurs in models with R -parity [7, 18] conservation. In viable realizations of the R -parity conserving MSSM, the LSP is a stable neutralino $\tilde{\chi}_1^0$, namely an electroweakino mass eigenstate composed of a mixture of bino, wino, and higgsino states. To be consistent with the observed DM relic density, a nearly pure wino (higgsino) LSP must have a mass of approximately 2 (1) TeV in such realizations [19]. The constraint arises from the value of the co-annihilation cross section required to sufficiently reduce the DM content of the early universe before thermal freeze-out [20, 21]. The co-annihilation cross section depends on the masses of the LSP and its co-annihilation partner. For a pure wino- or higgsino-like LSP, this partner is a chargino $\tilde{\chi}_1^\pm$ that is nearly degenerate in mass with the LSP, having a mass only a few hundred MeV larger. Because of the limited kinematic phase space in $\tilde{\chi}_1^\pm \rightarrow \tilde{\chi}_1^0 \pi^\pm$ decays, the $\tilde{\chi}_1^\pm$ then has a macroscopic lifetime, with a decay length at the LHC on the order of several centimeters or more.

Long-lived charginos associated with pure wino or higgsino DM give rise to the distinctive experimental signature known as a disappearing track (DTk). In $\tilde{\chi}_1^\pm \rightarrow \tilde{\chi}_1^0 \pi^\pm$ decays, the resulting pion has a momentum of only a few hundred MeV, too low, in general, for it to be reconstructed. The $\tilde{\chi}_1^0$ in these decays escapes undetected with most of the momentum. The chargino is reconstructed as a track with hits up to its point of decay, beyond which no hits or associated signals are recorded. This leads to the DTk signature in which a reconstructed track emanating from the beam collision region ends abruptly within the sensitive tracking volume, with a continuation that has “disappeared.” The DTk signature has been used in recent searches to set the most stringent chargino mass limits to date for certain scenarios, e.g., wino or higgsino LSP scenarios with minimal neutralino mixing [22–24].

This paper presents a search for long-lived charginos, probing a comprehensive set of final states relevant to the R -parity conserving MSSM. The analysis is based on a sample of proton-proton (pp) collision events collected at center-of-mass energy $\sqrt{s} = 13$ TeV with the CMS detector in 2016–2018, corresponding to an integrated luminosity of 137 fb^{-1} . It expands on previous searches [22, 23] by introducing electron+DTk and muon+DTk channels, by re-analyzing the fully hadronic channel, and by making use of a machine-learning-based track classification method to improve the DTk selection efficiency and background rejection. The addition of the electron+DTk and muon+DTk channels increases sensitivity to new-physics scenarios with leptonic final states. Additional sensitivity to high-mass LSP states is achieved by employing a measure of the dE/dx ionization energy loss of signal-candidate tracks, which takes large values for candidates with a small Lorentz boost. The analysis targets both the electroweak and strong production mechanisms, making use of jet and b -tagged jet multiplicities to distinguish between different production modes and decay chains. The incorporation of new final states and observables improves the sensitivity to relatively unexplored regions of the MSSM, including scenarios with pure wino or higgsino DM with masses of 1 TeV or larger, or with light third-generation squarks that yield leptons in the final state.

This paper is structured as follows. The signal models considered for the analysis are presented in Section 2. The CMS detector is described in Section 3 and the event reconstruction in Section 4. Section 5 discusses the simulated event samples used in the study. The DTK selection procedure is presented in Section 6 and the definition of the search regions (SRs) in Section 7. The methods used to estimate SM backgrounds are presented in Section 8. Systematic uncertainties are discussed in Section 9. The results and summary are presented in Sections 10 and 11, respectively. Tabulated results for the study are provided in the HEPData record for this analysis [25].

2 Simplified signal models

A number of simplified models of SUSY [26–28] are used to survey and characterize the sensitivity of the search. These models, depicted by representative production diagrams in Fig. 1 and summarized in Table 1, are effective-Lagrangian descriptions defined by the SUSY particle masses and the production and decay processes. A simplified model focuses on a specific small set of particles and interactions, with all other new-physics particles considered to be irrelevant to that particular process. One model, denoted T6btLL, features top squark pair production in which the top squark decays as $\tilde{t} \rightarrow t\tilde{\chi}_1^0$ and $\tilde{t} \rightarrow b\tilde{\chi}_1^\pm$, each with 50% probability. An analogous model with bottom squark production is labeled T6tbLL. A third model, denoted T5btbtLL, features gluino pair production in which the gluino decays as $\tilde{g} \rightarrow b\bar{b}\tilde{\chi}_1^0$, $\tilde{g} \rightarrow t\bar{t}\tilde{\chi}_1^0$, $\tilde{g} \rightarrow t\bar{b}\tilde{\chi}_1^+$, or $\tilde{g} \rightarrow \bar{t}b\tilde{\chi}_1^-$, each with 25% probability. Various proper decay lengths $c\tau$ of the chargino are considered. For the models with gluino and squark pair production, we focus on a benchmark model with $c\tau = 10$ cm, corresponding roughly to pure wino and higgsino-like states. We also consider a model with $c\tau = 200$ cm, which can be realized in a scenario with a bino-like LSP and a wino coannihilation partner. The chargino and LSP are required to be mass degenerate within a few hundred MeV. We set this mass difference to 180 MeV. This choice has no direct impact on the acceptance because the decay products of the chargino are not reconstructed.

Sensitivity to the direct production of either a nearly pure wino DM candidate or a nearly pure higgsino DM candidate is considered through the topologies denoted TChiWZ, TChiWW, and TChiW. The $\tilde{\chi}_2^0$ particle depicted for the TChiWZ diagram [Fig. 1 (lower left)] is the second lightest neutralino, only present in the higgsino scenario. Relationships among the electroweakino masses, the $\tilde{\chi}_1^\pm$ lifetime, and the $\tilde{\chi}_1^\pm$ decay width are constrained by radiative corrections that account for a large difference between the LSP mass and the SUSY-breaking scale. They are characterized in Refs. [29, 30] for the wino scenario and in Refs. [31, 32] for the higgsino scenario. The mass difference $\Delta m^0 = \Delta m(\tilde{\chi}_2^0, \tilde{\chi}_1^0)$ between the two neutral states is taken to be twice the mass difference $\Delta m^\pm = \Delta m(\tilde{\chi}_1^\pm, \tilde{\chi}_1^0)$ between the charged and lightest states. This choice corresponds to large $\tan\beta$, where $\tan\beta$ is the ratio of the vacuum expectation values of the neutral components of the two Higgs doublets in the MSSM [33]. The lifetime of the $\tilde{\chi}_2^0$, while not directly relevant for this study, is taken from a tree-level calculation based on the program SUSYHIT 1.5a [34]. The free parameters of the model are Δm^\pm and the chargino mass $m_{\tilde{\chi}_1^\pm}$.

3 The CMS detector and analysis triggers

The CMS detector is structured around a cylindrical superconducting solenoid with an inner diameter of 6 m. The solenoid provides a nearly uniform 3.8 T magnetic field within its volume. This volume contains a number of nested particle detectors: from the innermost region outward, a silicon pixel and strip tracking detector, a lead tungstate crystal electromagnetic

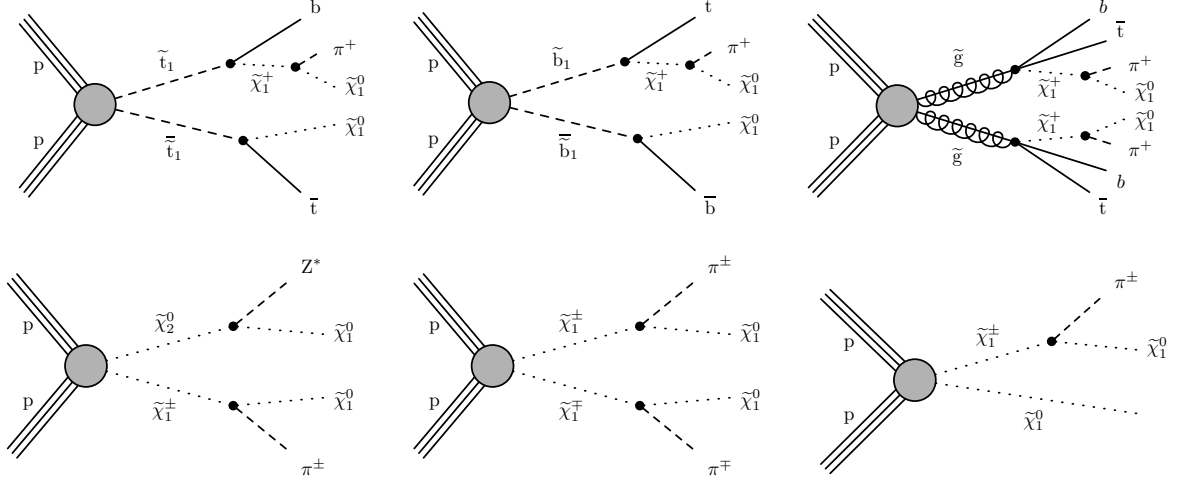


Figure 1: Representative diagrams for the simplified models considered in this analysis. From left to right: T6btLL, T6tbLL, and T5btbtLL (upper); and TChiWZ, TChiWW, and TChiW (lower). The shaded circles at the production vertices represent a sum over perturbative terms.

Table 1: Overview of the simplified models of supersymmetry considered in this analysis.

Model name	Description	Processes
T6btLL	Top squark associated $\tilde{\chi}_1^\pm$ production	$\tilde{t}\tilde{t}; \tilde{t} \rightarrow \tilde{t}\tilde{\chi}_1^0, \tilde{t} \rightarrow b\tilde{\chi}_1^\pm$
T6tbLL	Bottom squark associated $\tilde{\chi}_1^\pm$ production	$\tilde{b}\tilde{b}; \tilde{b} \rightarrow b\tilde{\chi}_1^0, \tilde{b} \rightarrow t\tilde{\chi}_1^\pm$
T5btbtLL	Gluino associated $\tilde{\chi}_1^\pm$ production	$\tilde{g}\tilde{g}; \tilde{g} \rightarrow b\tilde{b}\tilde{\chi}_1^0, \tilde{t}\tilde{t}\tilde{\chi}_1^0, \tilde{t}\tilde{b}\tilde{\chi}_1^-, \tilde{t}\tilde{b}\tilde{\chi}_1^+$
TChiWZ		$\tilde{\chi}_2^0\tilde{\chi}_1^\pm; \tilde{\chi}_2^0 \rightarrow Z^*\tilde{\chi}_1^0, \tilde{\chi}_1^\pm \rightarrow \tilde{\chi}_1^0\pi^\pm$
TChiWW	Electroweakino production for wino or higgsino LSP	$\tilde{\chi}_1^+\tilde{\chi}_1^-; \tilde{\chi}_1^\pm \rightarrow \tilde{\chi}_1^0\pi^\pm$
TChiW		$\tilde{\chi}_1^\pm\tilde{\chi}_1^0; \tilde{\chi}_1^\pm \rightarrow \tilde{\chi}_1^0\pi^\pm, \tilde{\chi}_1^0$

calorimeter (ECAL), and a brass and scintillator hadron calorimeter (HCAL). The ECAL and HCAL, each composed of a barrel and two endcap sections, cover the pseudorapidity range $|\eta| < 3.0$. Forward calorimeters extend the coverage to $3.0 < |\eta| < 5.2$. Muons are measured with gas-ionization detectors embedded in a steel flux-return yoke outside the solenoid, allowing muon reconstruction within $|\eta| < 2.4$. The CMS components taken together provide a nearly hermetic detector, permitting accurate measurements of the missing transverse momentum p_T^{miss} .

The tracking detector is of special importance for this analysis. The tracker consists of an inner pixel detector and an outer strip detector. The tracker used for the 2016 data-taking period, referred to as the ‘‘Phase-0’’ tracker, measured particles within $|\eta| < 2.5$. At the beginning of 2017, an upgraded pixel detector was installed [35]. The upgraded tracker is referred to as the ‘‘Phase-1’’ tracker. The Phase-1 tracker, used for the 2017 and 2018 data-taking periods, measured particles within $|\eta| < 3.0$. Tracks traversing the tracker system encounter 3 (4) pixel layers within a radius of 102 (160) mm in the Phase-0 (Phase-1) tracker. They encounter up to around 10 layers in the strip detector within a radius of 1.2 m. Compared to the Phase-0 tracker, the Phase-1 tracker provides improved tracking and vertex resolution, enhanced b-tagging performance, and a better measurement of the dE/dx track energy loss [35].

Events of interest are selected using a two-tiered trigger system [36]. The first level (L1), composed of custom hardware processors, uses information from the calorimeters and muon detectors to select events at a rate of around 100 kHz within a fixed latency of about $4 \mu\text{s}$ [37].

The second level, known as the high-level trigger, consists of a farm of processors running a version of the full event reconstruction software optimized for fast processing, and reduces the event rate to around 1 kHz before data storage [36]. For the hadronic DTk channel, signal event candidates were recorded by requiring p_T^{miss} at the trigger level to exceed a threshold that varied between 100 and 120 GeV, depending on the LHC instantaneous luminosity. For the electron+DTk (muon+DTk) channel, signal event candidates were recorded by requiring an electron (muon) candidate with $p_T > 27$ (24) GeV at the trigger level, where p_T is the transverse momentum. The trigger efficiencies are measured in data using independent cross triggers and are found to exceed 97% for events in the hadronic DTk channel and 80 (90)% for $p_T > 40$ GeV in the electron+DTk (muon+DTk) channel, for events that satisfy the selection criteria given below in Section 7.

A detailed description of the CMS detector, along with definitions of the coordinate system and kinematic variables, is given in Ref. [16].

4 Event reconstruction

Individual particles are reconstructed as particle-flow (PF) objects with the CMS PF algorithm [38], which identifies them as photons, charged hadrons, neutral hadrons, electrons, or muons. To improve the quality of the electron reconstruction, additional criteria (beyond those of the PF algorithm) are imposed on the $\sigma_{i\eta i\eta}$ variable [39], which is a measure of the width of the ECAL shower shape in the η coordinate, and on the ratio H/E of energies associated with the electron candidate in the HCAL and ECAL [39]. Specifically, small values of $\sigma_{i\eta i\eta}$ and H/E are required, with the criteria optimized separately for the barrel and endcaps [39]. For muon candidates, additional criteria are imposed on the matching between track segments reconstructed in the silicon tracker and muon detector [40]. Electron and muon candidates are required to have $p_T > 40$ GeV and $|\eta| < 2.4$.

The primary vertex (PV) is taken to be the vertex corresponding to the hardest scattering in the event, evaluated using tracking information alone as described in Section 9.4.1 of Ref. [41]. Charged-particle tracks associated with vertices other than the PV are removed from further consideration. The PV is required to lie within 24 cm of the center of the detector in the direction along the beam axis and within 2 cm in the plane transverse to that axis.

Jets are defined by clustering PF candidates using the anti- k_T jet algorithm [42, 43] with a distance parameter of 0.4. Jet quality criteria [44, 45] are imposed to eliminate jets from spurious sources such as electronics noise. The jet energies are corrected for the nonlinear response of the detector [46] and to account for the expected contributions of neutral particles from extraneous pp interactions (pileup) [47]. Jets are required to have $p_T > 30$ GeV, $|\eta| < 2.4$, and to not overlap with an identified lepton within a cone of radius $\Delta R \equiv \sqrt{(\Delta\phi)^2 + (\Delta\eta)^2} = 0.4$ around the jet direction, where ϕ is the azimuthal angle. The number of selected jets in an event is denoted N_{jet} .

The identification of b jets is performed by applying a version of the combined secondary vertex algorithm based on deep neural networks (DEEPCSV) [48] to the selected jet sample. The medium working point of this algorithm is used. The tagging efficiency for b jets with $p_T \approx 30$ GeV is 65%. The corresponding misidentification probability for gluon and light-quark (u, d, s) jets is 1.6%, while that for charm quark jets is 13%. The number of identified b jets in an event is denoted $N_{\text{b-jet}}$.

To suppress the contributions of jets erroneously identified as leptons as well as those due to

genuine leptons from hadron decays, electron and muon candidates are subjected to a lepton-isolation requirement. This isolation criterion is based on the variable I , which is the sum of the scalar p_T of charged hadron, neutral hadron, and photon PF candidates within a cone of radius ΔR around the lepton direction, divided by the lepton p_T . The expected contributions to this sum of neutral particles from pileup are subtracted [47]. The radius ΔR of the cone is 0.2 for lepton $p_T < 50$ GeV, $10 \text{ GeV}/p_T$ for $50 < p_T < 200$ GeV, and 0.05 for $p_T > 200$ GeV. The decrease in ΔR with increasing lepton p_T accounts for the increased collimation of the decay products from the lepton's parent particle as the Lorentz boost of the parent particle increases [49]. The isolation requirement is $I < 0.1$ (0.2) for electrons (muons).

The analysis uses a measure of the missing transverse momentum called the "hard p_T^{miss} " $p_{T,\text{hard}}^{\text{miss}}$, defined as the magnitude of the vector sum of \vec{p}_T over all PF jets with $p_T > 30$ GeV and $|\eta| < 5.0$, where the PF jets are defined as outlined above but are clustered inclusively, meaning that isolated leptons and photons are included as "jets." The lepton-isolation and jet-lepton overlap rejection criteria described above are not applied to jets used to compute $p_{T,\text{hard}}^{\text{miss}}$. Hard p_T^{miss} is more robust against pileup and soft radiation than the p_T^{miss} variable calculated through a sum over individual particles in an event rather than jets.

5 Simulated event samples

Simulated events are used to train boosted decision tree (BDT) multivariate binary classifiers and to estimate the signal acceptance in the SRs. The BDTs are used to help identify DTK candidates, as discussed in Section 6.

The SM production of $t\bar{t}$, W +jets, and Z +jets events, as well as of multijet events produced through quantum chromodynamics (QCD) processes, is simulated at leading order (LO) precision using the MADGRAPH5_aMC@NLO 2.2.2 [50, 51] event generator. The $t\bar{t}$ events are generated with up to three additional partons in the matrix element calculation. The W +jets and Z +jets events are generated with up to four additional partons. Single top quark events produced through the s channel, diboson events such as those originating from WW , ZZ , or ZH production (where H is the SM Higgs boson), and rare events such as those from $t\bar{t}W$, $t\bar{t}Z$, and WWZ production, are generated with the MADGRAPH5_aMC@NLO generator at next-to-leading order (NLO) [52], with the exception of WW events when both W bosons decay leptonically, which are generated with the POWHEG v2.0 [53–57] generator at NLO. This same POWHEG generator is used to describe single top quark event production through the t and tW channels. Normalization of the simulated background samples is based on the cross section calculations of Refs. [50, 56–66], which generally correspond to NLO or next-to-NLO (NNLO) precision. The detector response is based on the GEANT4 [67] suite of programs.

With the exception of the pure wino and higgsino models, simulated signal events are generated at LO using the MADGRAPH5_aMC@NLO generator, with up to two additional partons included. The production cross sections are determined with approximate NNLO plus next-to-next-to-leading logarithmic (NNLL) accuracy [68–79]. Events with gluino (squark) pair production are generated for a range of gluino $m_{\tilde{g}}$ (squark $m_{\tilde{q}}$) and LSP $m_{\tilde{\chi}_1^0}$ mass values, with $m_{\tilde{\chi}_1^0} < m_{\tilde{g}}$ ($m_{\tilde{\chi}_1^0} < m_{\tilde{q}}$). The ranges of mass considered vary according to the model, but are generally from around 600–2500 GeV for $m_{\tilde{g}}$, 200–1700 GeV for $m_{\tilde{q}}$, and 0–1500 GeV for $m_{\tilde{\chi}_1^0}$. The gluinos and squarks decay according to the phase space model of Ref. [80]. For the pure wino and higgsino models, simulated signal events are generated at LO using the PYTHIA 8.205 generator [80].

To render the computational requirements manageable, the detector response for signal events is based on the CMS fast simulation program [81, 82], which yields results that are generally consistent with those from GEANT4. To improve the consistency with GEANT4, we apply a correction of 1% to the fast simulation samples to account for differences in the efficiency of the jet quality requirements [44, 45] and corrections of 5–12% to account for differences in the b jet tagging efficiency. Additional corrections are applied to account for differences in the efficiency of tagging charginos with the Phase-0 and -1 trackers.

Parton showering and hadronization are simulated with the PYTHIA 8.205 generator [80]. For background events, the Phase-0 samples use the CUETP8M1 [83] tune while the Phase-1 samples use the CP5 [84] tune. For signal events, the CP2 [84] tune is used. Simulated samples generated at LO (NLO) with the CUETP8M1 tune use the NNPDF3.0LO (NNPDF3.0NLO) [85] parton distribution function (PDF). Those generated with the CP2 or CP5 tune use the NNPDF3.1LO (NNPDF3.1NNLO) [86] PDF.

To improve the MADGRAPH5_aMC@NLO modeling of the jet multiplicity from initial-state radiation (ISR), we follow the procedure introduced in Refs. [87, 88]. A control sample enriched in $t\bar{t}$ events is selected in both data and simulation by requiring two lepton candidates (ee , $\mu\mu$, or $e\mu$) and two tagged b jets. The number of all other jets in an event is denoted $N_{\text{jet}}^{\text{ISR}}$. Reweighting factors are applied to the simulated $t\bar{t}$ events so that the $N_{\text{jet}}^{\text{ISR}}$ distribution in simulation agrees with that in data. The same reweighting factors are also applied to the simulated signal events. The reweighting factors are 0.920, 0.821, 0.715, 0.662, 0.561, and 0.511 for $N_{\text{jet}}^{\text{ISR}} = 1, 2, 3, 4, 5$, and ≥ 6 , respectively.

6 Selection of disappearing track candidates

Two categories of DTK are defined: short tracks and long tracks. Short tracks have hits recorded only in the pixel detector. Long tracks have hits in both the pixel and strip detectors. The track p_T is required to exceed 25 (40) GeV for the short (long) category. The pseudorapidity is required to satisfy $|\eta| < 2.0$. This latter requirement reduces the background from spurious tracks (Section 8), which appears preferentially in the forward region. To ensure that the tracks are isolated, we calculate the relative isolation I_{rel} , defined by the sum of the scalar p_T of other tracks within a cone of radius $\Delta R = 0.3$ around the track direction, divided by the track p_T . We require $I_{\text{rel}} < 0.2$. The impact parameter d_{xy} of the track in the transverse plane and the impact parameter d_z in the direction along the beam axis must both be less than 0.1 cm, where d_{xy} and d_z are measured relative to the PV. The track is required to have at least three hits, one of which must be on the innermost pixel layer. Studies of simulated data show that charginos that decay within the tracker are rarely reconstructed as PF candidates. We therefore require the track to lie at least $\Delta R = 0.01$ away from any reconstructed particle and at least $\Delta R = 0.4$ away from any reconstructed jet with $p_T > 15$ GeV.

To select tracks that are consistent with a DTK, long tracks are required to not have hits in the outermost two layers of the strip detector, while short tracks are required to not have any hits whatsoever in the strip detector. In addition, tracks must not be identified as an electron, muon, or hadron. To ensure that DTK candidates are not associated with a large deposit of calorimetric energy, we calculate the quantity E_{dep} , which is the sum of ECAL and HCAL cluster energies deposited within $\Delta R = 0.4$ of the candidate track. Different criteria on E_{dep} and E_{dep}/p (with p the track momentum) are used to define SRs and control regions (CRs) for short and long tracks, respectively, and for the Phase-0 and -1 detectors, as indicated in Table 2. We use E_{dep}/p for long tracks because the resulting signal distribution peaks near 1, which is convenient for the

Table 2: Selection criteria on the BDT classifier score and on the calorimetric energy E_{dep} associated with a disappearing track candidate for the search region (SR) and control region (CR) samples discussed in Section 8.

Phase/category	Phase 0/short	Phase 0/long	Phase 1/short	Phase 1/long
BDT for SR samples	>0.1	>0.12	>0.15	>0.08
E_{dep} for SR samples	<15 GeV	<0.2 p	<15 GeV	<0.2 p
E_{dep} for CR ^{genuine} samples	[30, 300] GeV	[0.3, 1.2] p	[30, 300] GeV	[0.3, 1.2] p
BDT for CR ^{genuine} samples	>0.1	>0.05	>0.05	>0.08
BDT for CR ^{spurious} samples	[-0.10, -0.05]	[-0.1, 0.0]	[-0.10, 0.05]	[-0.1, 0.0]

selection process. However, because the uncertainty in p is larger for short tracks, the E_{dep}/p distribution for short tracks does not exhibit a clear peak, making it simpler to use E_{dep} . (The momentum resolution for long tracks is 10% or better, while for short tracks it is 20% or worse, depending on the number of hits associated with the track.) To further reduce background from electrons, additional criteria are applied to reject tracks that enter detector regions with an ECAL crystal with anomalously low light yield, a disabled crystal, or a noisy channel. These additional criteria reduce the signal efficiency by less than 2%.

A BDT classifier is used to improve the purity of the DTk candidate sample. For the signal training, chargino-matched tracks from simulated gluino and top squark pair-production events are used. The matching criterion is $\Delta R(\text{track}, \tilde{\chi}_{1,\text{gen}}^\pm) < 0.01$, where $\tilde{\chi}_{1,\text{gen}}^\pm$ represents a generator-level chargino. For the background training, tracks from all simulated SM processes are used. The input variables to the classifier are d_{xy} , d_z , I_{rel} , $\Delta p_T/p_T^2$, χ^2/n_d (with Δp_T the uncertainty in the reconstructed p_T value and n_d the number of degrees of freedom), the number of pixel hits, and, for long tracks, the number of strip hits and the number of missing outer strip hits, where this latter quantity is the number of strip layers between the outermost strip hit and the outermost strip layer for which no hit is recorded. Separate BDTs are trained for the short- and long-track categories and for the Phase-0 and -1 detectors. Distributions of the BDT output scores for these categories are shown in Fig. 2. Thresholds on the classifier output values are applied in defining SRs and CRs for the Phase-0 and -1 detectors, as indicated in Table 2. The classifier significantly improves the selection performance compared to so-called ‘‘cut-based’’ approaches, increasing the signal efficiency for short tracks by a factor ranging from 2 to 4, depending on the data-taking period, and of long tracks by around 50%, for an equivalent background rejection.

These requirements select 45 to 55% of charginos that decay after the second tracker layer and before the penultimate one, depending on the length of the track.

A novel technique is used to validate the DTk selection efficiency. First, well reconstructed, isolated muons are selected from both data and simulation. Tracker hits associated with the muon are iteratively removed from the event one-by-one, starting with the outermost hit and working inward, until only three tracker hits remain. These shortened track segments are used as a proxy for long-lived charged particles. After each step in the process, the complete event reconstruction procedure is reapplied and the efficiency for the tracking algorithm and DTk classifier to identify the shortened segments as a DTk candidate is determined. This efficiency ranges from 45 to 55% depending on the length of the shortened muon track, similar to the reconstruction efficiency for charginos mentioned above. The procedure is applied to samples corresponding to the various data-taking periods. Comparisons of the results between data and simulation are used to derive scale factors that are applied to the DTk selection efficiencies

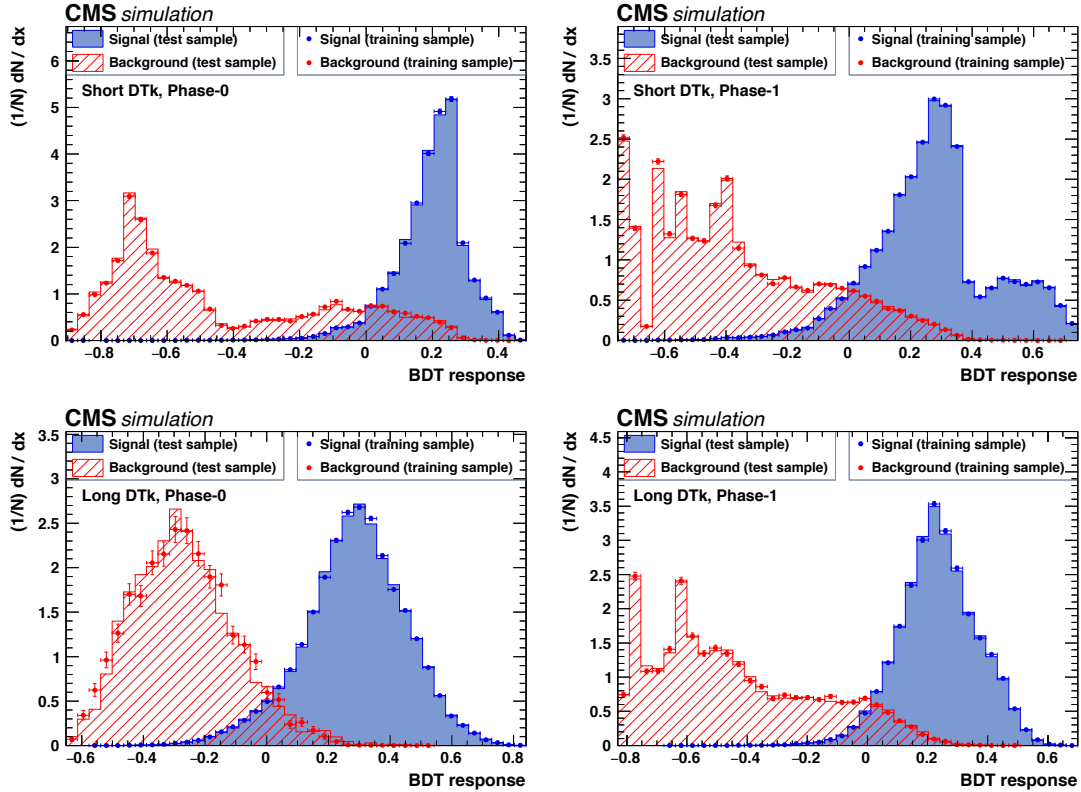


Figure 2: The distributions of simulated events used to train and validate the BDT classifiers. The left (right) column corresponds to the Phase-0 (Phase-1) detector and the upper (lower) row to the short (long) track category. The uncertainty bars shown for the training samples indicate the Poisson uncertainties. No events appear outside of the regions shown.

from simulation. The scale factors are consistent with unity with uncertainties, of statistical origin, that vary between 10 and 17%.

The DTK candidates are further classified on the basis of their dE/dx energy loss value in the pixel detector. As the measure of the dE/dx , we use the so-called “harmonic-2” hit-weighted average I_h [89, 90], which is an estimate of the linear stopping power of a particle that is robust with respect to outlier measurements. The I_h variable is defined by

$$I_h = \left(\frac{1}{N} \sum_{i=1}^N (\Delta E / \Delta x)_i^{-2} \right)^{-1/2}, \quad (1)$$

where ΔE is the energy loss estimated from the charge collected by a pixel hit, Δx is the length of the track segment corresponding to that hit, and N is the number of pixel hits on the track. We define two intervals in I_h : $I_h < 4.0$ and $I_h > 4.0$ MeV/cm. In the following, the term “ dE/dx ” refers to the I_h value.

Time-dependent calibration of the dE/dx measurement is performed in data using the position of the center of a Gaussian fit to the minimum-ionizing-particle peak of well-reconstructed muons, separately for the barrel and endcap regions. The dE/dx values from all data-taking periods are scaled to be consistent with the result from simulation, with a fit mean of 2.87 MeV/cm.

The dE/dx value can further be used to estimate the mass of the DTK, through the relation

(with m the charged-particle mass)

$$dE/dx = K \frac{m^2}{p^2} + C, \quad (2)$$

which is valid for singly charged particles [89]. The constants K and C are determined as described in Ref. [90] to be 2.684 ± 0.001 and 3.375 ± 0.001 MeV/cm, respectively. We refer to the DTK mass value determined in this manner as $m_{\text{DTk}; dE/dx}$. We do not use the $m_{\text{DTk}; dE/dx}$ variable for quantitative purposes but merely examine its distribution in Section 10.

7 Event selection and search regions

The number of DTK candidates in an event is denoted N_{DTk} . Signal events are required to have $N_{\text{DTk}} \geq 1$, $N_{\text{jet}} \geq 1$, and $p_{\text{T,hard}}^{\text{miss}} > 30$ GeV. At least one DTK candidate must satisfy $m_{\text{T}}(\text{DTk}, p_{\text{T,hard}}^{\text{miss}}) > 20$ GeV, where m_{T} is the transverse mass [91] formed from the two quantities in parentheses. For $N_{\text{DTk}} = 1$, the search is performed inclusively in the hadronic DTK, electron+DTk, and muon+DTk channels. We also search in a channel with $N_{\text{DTk}} \geq 2$. For this latter channel, events are required to satisfy the hadronic trigger requirements in the case of zero leptons or the trigger requirements for the electron (muon) channel in the case of $N_e \geq 1$ ($N_\mu \geq 1$), where N_e (N_μ) is the number of electron (muon) candidates in an event. The different search channels are defined as follows.

- Hadronic channel:
 - $N_{\text{DTk}} = 1$,
 - $N_e = N_\mu = 0$,
 - $p_{\text{T,hard}}^{\text{miss}} > 150$ GeV.
- Muon channel:
 - $N_{\text{DTk}} = 1$,
 - $N_e = 0$,
 - $N_\mu \geq 1$,
 - $m_{\text{DTk},\mu} > 120$ GeV,
 - $m_{\text{T}}(\mu, p_{\text{T,hard}}^{\text{miss}}) > 110$ GeV.
- Electron channel:
 - $N_{\text{DTk}} = 1$,
 - $N_e \geq 1$,
 - $m_{\text{DTk},e} > 120$ GeV,
 - $m_{\text{T}}(e, p_{\text{T,hard}}^{\text{miss}}) > 110$ GeV.
- $N_{\text{DTk}} \geq 2$ channel:
 - Satisfies the criteria given above for either the hadronic, muon, or electron channel, except for the N_{DTk} requirement,
 - $N_{\text{DTk}} \geq 2$.

The invariant mass $m_{\text{DTk},\ell}$ is formed from the DTK and the highest p_{T} electron or muon candidate in the event. The $m_{\text{DTk},\ell}$ and m_{T} requirements suppress the Drell-Yan (DY) and W+jets backgrounds, respectively. For the $m_{\text{DTk},\ell}$ calculation, the mass of the DTK is assumed to be zero. Note that we require $N_e = 0$ for the muon channel in order to render it orthogonal to the electron channel, but do not require $N_\mu = 0$ for the electron channel because it is unnecessary for the analysis.

Table 3: Definition of the search regions (SRs) for the hadronic channel.

Hadronic channel ($N_{\text{DTk}} = 1, N_{\mu} = 0, N_e = 0$)						
$p_{\text{T,hard}}^{\text{miss}}$ (GeV)	$N_{\text{b-jet}}$	N_{jet}	N_{short}	N_{long}	dE/dx (MeV/cm)	SR
150–300	0	1–2	0	1	<4.0	1
			>4.0	2		
		1	0	0	<4.0	3
			>4.0	4		
		≥ 3	0	1	<4.0	5
			>4.0	6		
	1	0	0	<4.0	7	
		>4.0	8			
	≥ 1	1–2	0	1	<4.0	9
			>4.0	10		
			1	0	<4.0	11
			>4.0	12		
		≥ 3	0	1	<4.0	13
			>4.0	14		
			1	0	<4.0	15
			>4.0	16		
>300	Any	1–2	0	1	<4.0	17
			>4.0	18		
		1	0	<4.0	19	
		>4.0	20			
	≥ 3	0	1	<4.0	21	
		>4.0	22			
		1	0	<4.0	23	
		>4.0	24			

The above requirements define the global SR, referred to as the “baseline” region. Events in the baseline region are divided into nonoverlapping SRs as follows. Events with $N_{\text{DTk}} = 1$ are sorted into 48 SRs based on the DTk length category, the dE/dx interval, and the values of N_{jet} , $N_{\text{b-jet}}$, and $p_{\text{T,hard}}^{\text{miss}}$. The choice of binning is designed to provide sensitivity to a wide range of scenarios, covering strong and electroweak production and the presence of all three generations of fermions. Events with $N_{\text{DTk}} \geq 2$ are grouped into a single SR, bringing the total number of SRs to 49. The definition of the SRs is given in Tables 3 and 4.

8 Background estimation

Disappearing track signatures are rare in the SM but can occasionally arise because of an instrumental effect, either from the misreconstruction of a charged particle or from the coincidental alignment of hits from different tracks. We refer to these backgrounds as the “genuine-particle” background and the “spurious-particle” background, respectively. We use methods based entirely on data to evaluate these backgrounds, as described below. These methods employ the so-called “ABCD” technique, for which a basic description is given in Ref. [92].

8.1 Genuine-particle background

In a typical case, genuine-particle background might arise from a track that showers in a crack between ECAL crystals or into a crystal with anomalously low light yield, yielding a signifi-

Table 4: Definition of the search regions (SRs) for the muon, electron, and $N_{\text{DTk}} \geq 2$ channels.

Muon channel ($N_{\text{DTk}} = 1, N_{\mu} \geq 1, N_e = 0$)						
$p_{\text{T,hard}}^{\text{miss}}$ (GeV)	$N_{\text{b-jet}}$	N_{jet}	N_{short}	N_{long}	dE/dx (MeV/cm)	SR
30–100	0	≥ 1	0	1	<4.0	25
					>4.0	26
			1	0	<4.0	27
					>4.0	28
	≥ 1		0	1	<4.0	29
					>4.0	30
			1	0	<4.0	31
					>4.0	32
>100	Any	0	1	<4.0	33	
				>4.0	34	
		1	0	<4.0	35	
				>4.0	36	
Electron channel ($N_{\text{DTk}} = 1, N_e \geq 1$)						
30–100	0	≥ 1	0	1	<4.0	37
					>4.0	38
			1	0	<4.0	39
					>4.0	40
	≥ 1		0	1	<4.0	41
					>4.0	42
			1	0	<4.0	43
					>4.0	44
>100	Any	0	1	<4.0	45	
				>4.0	46	
		1	0	<4.0	47	
				>4.0	48	
$N_{\text{DTk}} \geq 2$ channel						
>30	Any	≥ 1	Any			49

cantly undermeasured deposited energy that degrades the consistency between the measured track p_{T} and associated calorimetric energy, leading to a failure in the PF particle reconstruction. In other cases, a particle might emit a highly energetic photon, causing a recoil that similarly degrades this consistency. Concomitantly, the two outermost layers of the silicon tracker may not have hits associated with the track, which can arise through rare inefficiencies or from misassociation of hits in the strip detector. We refer to this type of background as the “genuine-particle showering” background. Less often, genuine-particle background can arise from a muon if there is a large or otherwise anomalous occupancy in the muon system or as a result of a rare misalignment between the track segment in the tracker with that in the muon system, again in conjunction with missing hits in the two outermost layers of the silicon tracker. We refer to this background as the “genuine-particle muon” background. These genuine-particle backgrounds represent the dominant background for the long-track category of DTks.

The genuine-particle showering background is evaluated using sideband control regions $\text{CR}^{\text{genuine}}$, one for each SR, and a separate “DY measurement” CR of Drell-Yan events. The $\text{CR}^{\text{genuine}}$ samples are defined by the intervals in E_{dep} and the BDT classifier listed in the third and fourth rows of Table 2. These criteria yield a high purity for genuine-particle showering events and thus negligible contamination. The $\text{CR}^{\text{genuine}}$ samples are selected using a loosened

Table 5: The transfer factors $\kappa_{\text{high}}^{\text{low}}$ and $\kappa_{\mu\text{match}}^{\mu\text{veto}}$ used for the evaluation of the genuine-particle backgrounds. The ‘‘Genuine shower’’ columns refer to the $\kappa_{\text{high}}^{\text{low}}$ factors while the ‘‘Genuine muon’’ columns refer to the $\kappa_{\mu\text{match}}^{\mu\text{veto}}$ factors. The genuine-particle muon background is negligible for the short category of DTks. The uncertainties are statistical only.

$\kappa_{\text{high}}^{\text{low}}, \kappa_{\mu\text{match}}^{\mu\text{veto}}$	Phase 0		Phase 1		Combined Phase 0 and 1	
	Genuine shower	Genuine muon	Genuine shower	Genuine muon	Genuine shower	Genuine muon
Short	0.65 ± 0.11	—	0.435 ± 0.049	—	0.492 ± 0.046	—
Long	0.247 ± 0.020	0.00099 ± 0.00017	0.389 ± 0.032	0.00047 ± 0.00012	0.307 ± 0.018	0.00074 ± 0.00011

isolation requirement on the DTks compared to the SRs. Specifically, the DTk candidate must only lie at least $\Delta R = 0.1$ away from any reconstructed jet with $p_T > 15$ GeV, rather than at least $\Delta R = 0.4$ as in Section 6. The reason for this loosened restriction is to increase the statistical precision of the background estimate. Other than these differences, the criteria used to select the $\text{CR}^{\text{genuine}}$ samples are the same as for the SR samples.

The DY measurement CR is selected by requiring events to contain an electron and a DTk candidate of opposite charge. The DTk candidate must satisfy the selection criteria for either the SR or $\text{CR}^{\text{genuine}}$ samples. The invariant mass $m(\text{DTk}, e)$ formed from the DTk and electron must be consistent with a Z boson, namely lie in a range from 65 to 110 GeV. For this calculation, the DTk is assigned a mass of zero. To improve the purity, we require $m_T(e, p_{T,\text{hard}}^{\text{miss}}) < 100$ GeV and that there be a relatively small difference $\Delta\phi$ in the azimuthal angle between the DTk and $p_{T,\text{hard}}^{\text{miss}}$: $\Delta\phi < \pi/2$ for long tracks and $\Delta\phi < \pi/4$ for short tracks. The $\Delta\phi$ requirement is imposed because genuine-particle DTks correspond to particles that are not reconstructed, which can lead to significant $p_{T,\text{hard}}^{\text{miss}}$ along the direction of the DTk.

A transfer factor $\kappa_{\text{high}}^{\text{low}}$ is derived from the DY measurement CR, given by the ratio of the number of events with small and large values of the f_{dep} variable,

$$\kappa_{\text{high}}^{\text{low}} = N_{f_{\text{dep}}^{\text{low}}}^{\text{DY}} / N_{f_{\text{dep}}^{\text{high}}}^{\text{DY}}, \quad (3)$$

where $f_{\text{dep}} = E_{\text{dep}}/p$ for long tracks and $f_{\text{dep}} = E_{\text{dep}}$ for short tracks. The E_{dep} requirements for the $f_{\text{dep}}^{\text{low}}$ ($f_{\text{dep}}^{\text{high}}$) region are the same as those listed for the SR ($\text{CR}^{\text{genuine}}$) samples in Table 2. The transfer factor is determined separately for short and long tracks and for the Phase-0 and -1 detectors. The DY measurement CR is nearly 100% pure in genuine-particle showering events except for the short-track category at low f_{dep} , where approximately 50% of the events arise from spurious tracks. The spurious-track contamination in this sample is evaluated using the method described in Section 8.2 and is then subtracted before the $\kappa_{\text{high}}^{\text{low}}$ factors are calculated, with an associated systematic uncertainty evaluated as described in Section 9. The values of the $\kappa_{\text{high}}^{\text{low}}$ factors are reported in the ‘‘Genuine shower’’ columns of Table 5.

The estimate $N_{\text{SR}_i}^{\text{genuine}}$ of the number of genuine-particle showering background events in the i th SR is

$$N_{\text{SR}_i}^{\text{genuine}} = \kappa_{\text{high}}^{\text{low}} N_{\text{CR}_i^{\text{genuine}}}, \quad (4)$$

with $N_{\text{CR}_i^{\text{genuine}}}$ the number of events in the i th $\text{CR}^{\text{genuine}}$ sample.

An analogous procedure is employed to evaluate the much smaller genuine-particle muon background, making use of sideband control regions $\text{CR}^{\text{genuine}-\mu}$ defined analogously to the SRs but inverting the requirement from Section 6 that the DTk not be identified as a PF muon, namely the track *must* be identified as a muon. We call this track a ‘‘DTk-proxy’’ track. A DY

measurement CR is defined in the same manner as described above for the genuine-particle showering background except with the Z boson candidate formed from a muon and the DTk-proxy track. The $CR^{\text{genuine-}\mu}$ and this DY measurement CR are essentially 100% pure in genuine-particle muon events and thus have negligible contamination. A transfer factor $\kappa_{\mu \text{ match}}^{\mu \text{ veto}}$ is derived from the DY measurement CR as the ratio of the number of events with the muon veto of Section 6 applied to the corresponding number with the veto inverted. The values of the transfer factors $\kappa_{\mu \text{ match}}^{\mu \text{ veto}}$ are listed in the ‘‘Genuine muon’’ columns of Table 5. Note that this background is negligible for short tracks because of the high efficiency of the combined strip tracker and muon systems.

The estimate $N_{\text{SR}_i}^{\text{genuine-}\mu}$ of the number of genuine-particle muon background events in the i th SR is

$$N_{\text{SR}_i}^{\text{genuine-}\mu} = \kappa_{\mu \text{ match}}^{\mu \text{ veto}} N_{\text{CR}_i^{\text{genuine-}\mu}}, \quad (5)$$

with $N_{\text{CR}_i^{\text{genuine-}\mu}}$ the number of events in the i th $CR^{\text{genuine-}\mu}$ sample.

We study the dependence of the transfer factors $\kappa_{\text{high}}^{\text{low}}$ and $\kappa_{\mu \text{ match}}^{\mu \text{ veto}}$ on the kinematic properties of the tracks. It is found that the p_T spectra of DTks in the DY measurement CRs are predicted reasonably well, with statistically significant deviations within 20% for the showering background tracks. Comparisons between the predicted and observed p_T spectra of the tracks in the two DY measurement CRs are presented in Fig. 3. Tests of the method are performed in high- m_T validation regions defined in the same manner as the corresponding DY measurement CR but with the inverted requirement $m_T > 110 \text{ GeV}$. The results in the validation regions are shown in Fig. 4 and indicate agreement between the predicted and observed results to within the statistical and systematic uncertainties.

8.2 Spurious-particle background

The spurious-particle background arises when hits in the silicon tracker from two or more particles align to form a pattern that mimics the signature of a single particle. Such combinatoric patterns typically do not have associated calorimetric or muon system activity. They thereby can satisfy the selection criteria for DTks and appear as background in our search. The spurious-particle background depends primarily on the level of activity in an event, particularly the occupancy of the tracker. It forms the dominant background for the short-track category of DTks.

The spurious-particle background is evaluated using sideband control regions CR^{spurious} , one for each SR, and a ‘‘QCD measurement CR’’ enhanced in QCD multijet events. The CR^{spurious} samples are selected using the same criteria as for the corresponding SRs except with lower ranges in the BDT variable. These ranges are listed in the last row of Table 2. The ranges are chosen so as to yield sufficiently populated samples, a high purity of spurious tracks, and a phase space similar to the SRs.

The QCD measurement CR is selected by requiring $N_e = N_\mu = N_{\text{b-jet}} = 0$ and $30 < p_{T,\text{hard}}^{\text{miss}} < 60 \text{ GeV}$. It is essentially 100% pure in spurious-track events, with negligible contamination. A transfer factor $\theta_{\text{low}}^{\text{high}}$ is derived from the QCD measurement CR sample as

$$\theta_{\text{low}}^{\text{high}} = N_{\text{BDT}^{\text{high}}}^{\text{QCD}} / N_{\text{BDT}^{\text{low}}}^{\text{QCD}}, \quad (6)$$

with $N_{\text{BDT}^{\text{high}}}^{\text{QCD}}$ and $N_{\text{BDT}^{\text{low}}}^{\text{QCD}}$ the number of events satisfying the BDT selection criteria in Table 2 for the SR and CR^{spurious} selections, respectively. The values of the transfer factors $\theta_{\text{low}}^{\text{high}}$ are

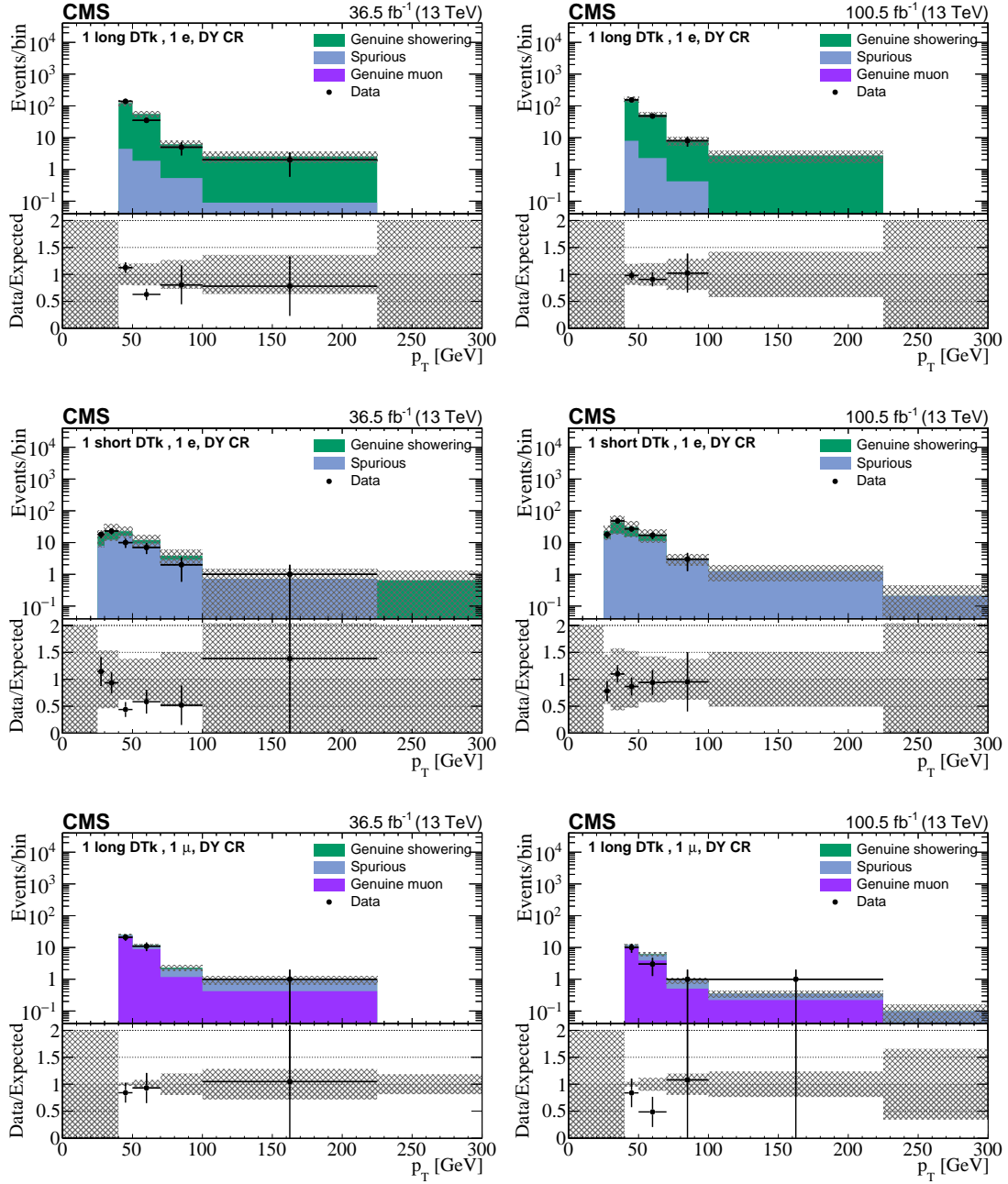


Figure 3: Comparison of the p_T distributions of DTKs in the $\kappa_{\text{high}}^{\text{low}}$ DY measurement control region for the data and background prediction for long (upper) and short (middle) showering tracks and in the $\kappa_{\mu \text{ match}}^{\mu \text{ veto}}$ DY measurement control region for long muon tracks (lower). The left (right) column corresponds to the Phase-0 (Phase-1) detector. The uncertainty bars on the ratios in the lower panels indicate the fractional Poisson uncertainties in the observed counts. The gray bands show the fractional Poisson uncertainties in the sideband region counts, added in quadrature with the systematic uncertainties. The leftmost (rightmost) bin includes underflow (overflow).

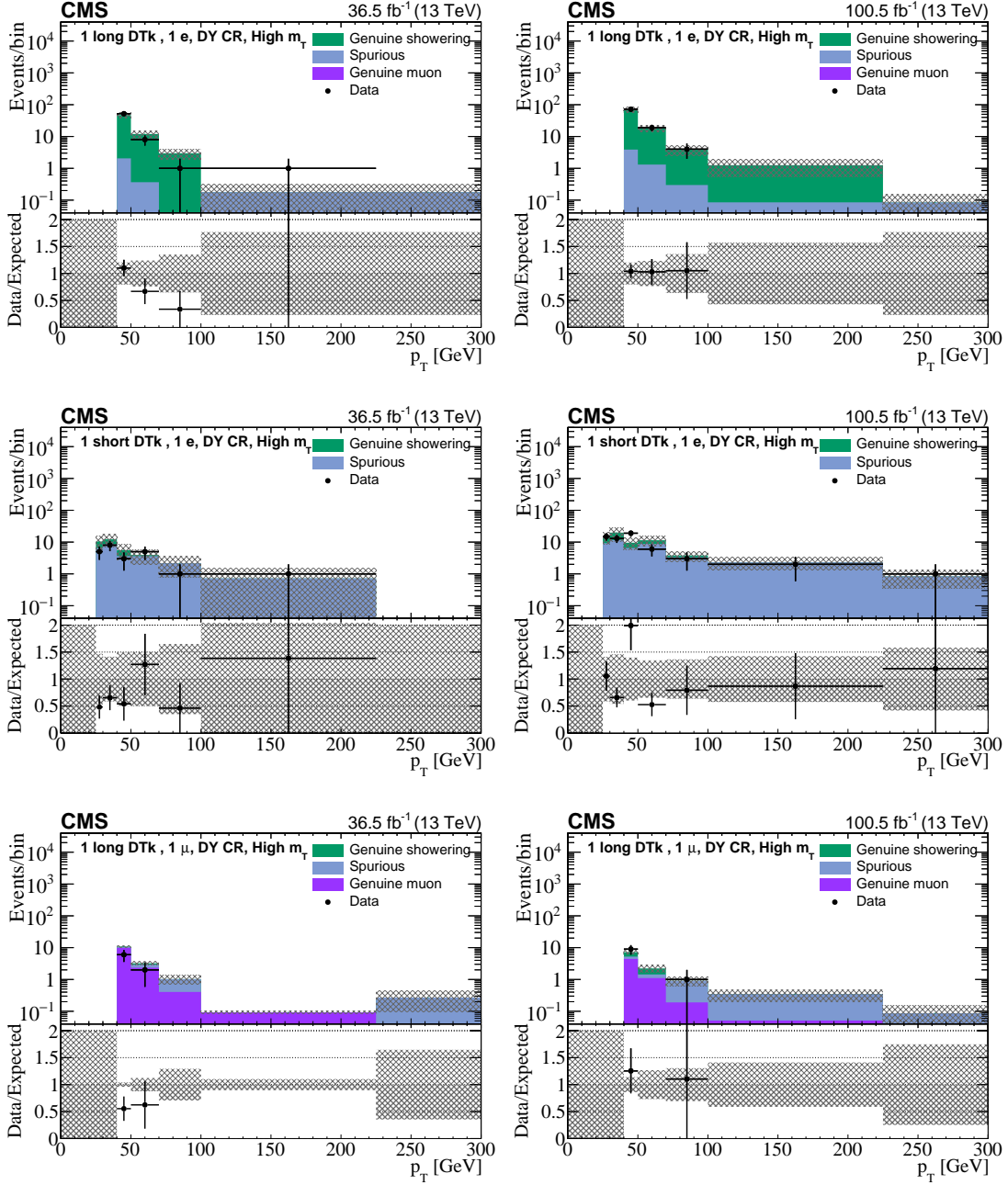


Figure 4: Comparison of the p_T distributions of DTks in the high- m_T validation region for the data and background prediction for long (upper) and short (middle) showering tracks and for long muon tracks (lower). The left (right) column corresponds to the Phase-0 (Phase-1) detector. The uncertainty bars on the ratios in the lower panels indicate the fractional Poisson uncertainties in the observed counts. The gray bands show the fractional Poisson uncertainties in the sideband region counts, added in quadrature with the systematic uncertainties. The leftmost (rightmost) bin includes underflow (overflow).

Table 6: The transfer factor $\theta_{\text{low}}^{\text{high}}$ used for the evaluation of the spurious-particle background. The uncertainties are statistical only.

$\theta_{\text{low}}^{\text{high}}$:	Spurious particle		
	Phase 0	Phase 1	Combined Phase 0 and 1
Short	0.722 ± 0.079	0.210 ± 0.020	0.346 ± 0.025
Long	0.089 ± 0.015	0.042 ± 0.021	0.080 ± 0.013

listed in Table 6.

The estimate $N_{\text{SR}_i}^{\text{spurious}}$ of the number of spurious-particle background events in the i th SR is

$$N_{\text{SR}_i}^{\text{spurious}} = \theta_{\text{low}}^{\text{high}} N_{\text{CR}_i^{\text{spurious}}}, \quad (7)$$

with $N_{\text{CR}_i^{\text{spurious}}}$ the number of events in the i th CR^{spurious} event sample.

Because of the limited size of the data sample, six SRs in the large dE/dx category have no events in the corresponding CR^{spurious} sample: these are bins 18, 22, 34, 42, 44, and 46 (see Tables 3 and 4). To obtain a prediction for these bins, an extrapolation is made based on the predicted spurious-track background in the adjacent SR, namely, the equivalent SR in the low dE/dx category. The prediction is made as

$$(N_{\text{SR}_i}^{\text{spurious}})_{dE/dx\text{-high}} = \phi_{\text{low}}^{\text{high}} (N_{\text{SR}_i}^{\text{spurious}})_{dE/dx\text{-low}}, \quad (8)$$

where the transfer factor $\phi_{\text{low}}^{\text{high}}$ is studied in various CRs and is found to be 0.18 ± 0.05 for both long and short tracks, independent of any analysis variable. Relative systematic uncertainties associated with the extrapolated counts are taken from the bin from which the value is extrapolated, in addition to the uncertainty in $\phi_{\text{low}}^{\text{high}}$.

Comparisons between the predicted and observed p_T spectra of DTk candidates in the QCD measurement CR are shown in Fig. 5. The spectra are seen to be reasonably well modeled, with statistically significant deviations below around 30%, within the total uncertainty. Tests of the spurious-particle background evaluation procedure are performed in a validation region defined by requiring the presence of one electron and one DTk, with the restrictions $m_T < 110$ GeV and $m_{\text{DTk},\ell} \notin [65, 110]$ GeV. Note that this validation region also accounts for genuine-particle background that might be present in the spurious-particle sample. The results, shown in Fig. 6, again demonstrate general agreement within the uncertainties.

9 Systematic uncertainties

We consider the following sources of systematic uncertainty in the signal event yields. Nuisance parameters associated with systematic uncertainties are treated as correlated across all search bins.

- *DTk selection efficiency*: The uncertainty in the DTk selection efficiency is taken to be the uncertainty in the DTk selection efficiency scale factors mentioned in Section 6.
- *Integrated luminosity*: The systematic uncertainty in the determination of the integrated luminosity is 1.6% [93–96].
- *Jet energy scale and resolution*: Uncertainties in the jet energy scale and resolution are evaluated as a function of jet p_T and η , and propagated to higher level quantities such as N_{jet} and $p_{T,\text{hard}}^{\text{miss}}$ [45, 46, 97].

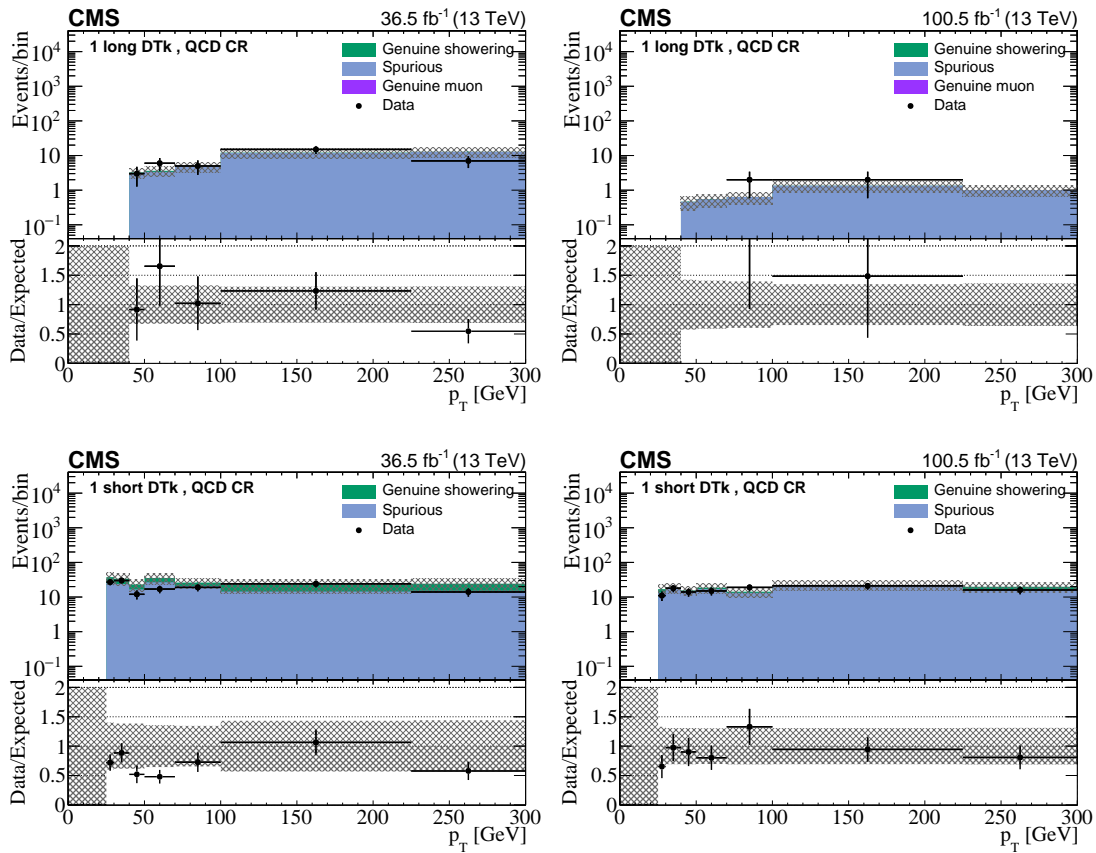


Figure 5: Comparison of the p_T distributions of DTks in the $\theta_{\text{low}}^{\text{high}}$ QCD measurement control region for the data and background prediction for long (upper) and short (lower) tracks. The left (right) column corresponds to the Phase-0 (Phase-1) detector. The uncertainty bars on the ratios in the lower panels indicate the fractional Poisson uncertainties in the observed counts. The gray bands show the fractional Poisson uncertainties in the control region counts, added in quadrature with the systematic uncertainties. The leftmost (rightmost) bin includes underflow (overflow).

- *b jet tagging efficiency and mistagging*: p_T , η , and flavor-dependent uncertainties in the b jet tagging and light-quark jet mistagging scale factors, accounting both for data-versus-GEANT4-simulation differences and for GEANT4-versus-fast-simulation differences, are derived from control samples of $t\bar{t}$ and QCD multijet events.
- *Renormalization and factorization scales*: Uncertainties associated with the renormalization (μ_R) and factorization (μ_F) scales are evaluated by independently varying μ_R and μ_F by a factor of 2.0 and 0.5 [98–100].
- *Initial-state radiation*: The uncertainty in the modeling of initial-state radiation is taken to be one half of the deviation from unity in the ISR reweighting factors presented in Section 5.
- *Pileup modeling*: The uncertainty associated with pileup reweighting is evaluated by varying the value of the total inelastic cross section by 4.6% [101] from its nominal value of 69.2 mb.
- *Trigger efficiency*: The uncertainty in the trigger efficiency of the hadronic channel is assessed from its observed dependence on jet multiplicity and of the leptonic channels from the observed difference relative to an alternative trigger. In addition, the

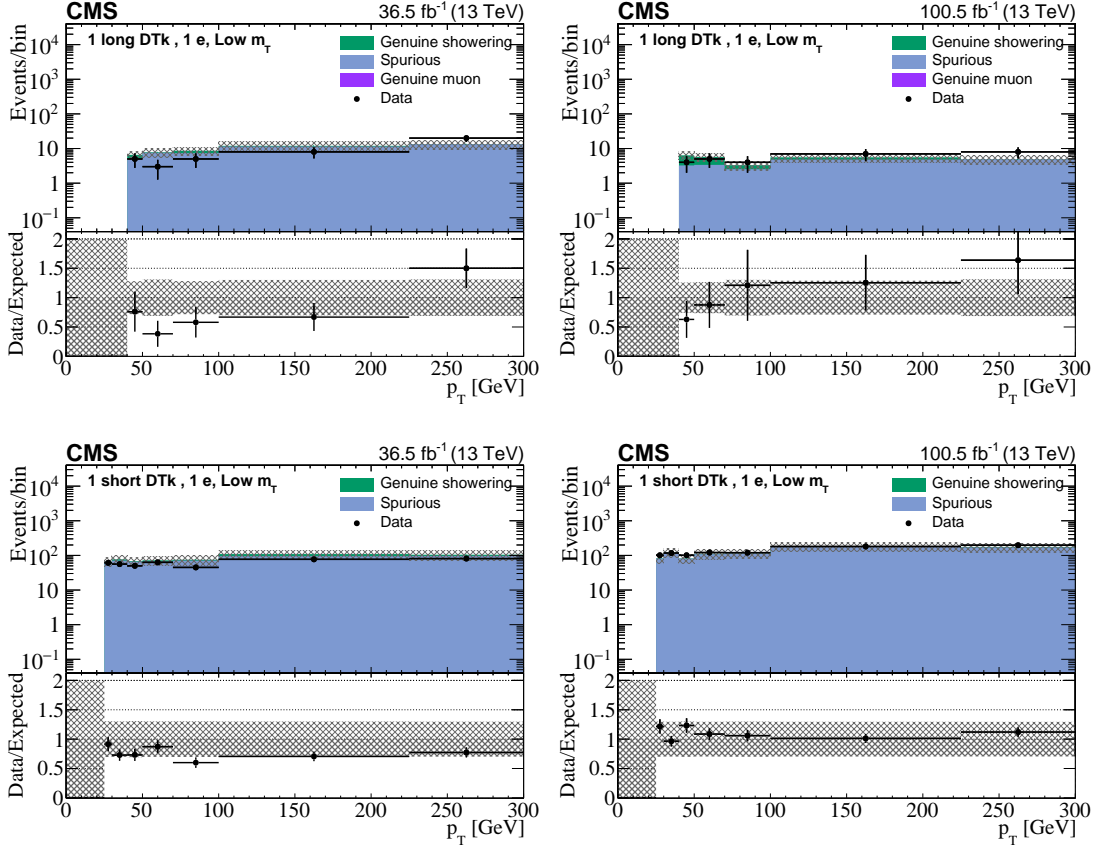


Figure 6: Comparison of the p_T distributions of DTKs in events with one electron and one DTK, in a validation region with $m_T < 110$ GeV and $m_{\text{DTK},\ell} \notin [65, 110]$ GeV, for the data and background prediction for long (upper) and short (lower) tracks. The left (right) column corresponds to the Phase-0 (Phase-1) detector. The uncertainty bars on the ratios in the lower panels indicate the fractional Poisson uncertainties in the observed counts. The gray bands show the fractional Poisson uncertainties in the control region counts, added in quadrature with the systematic uncertainties. The leftmost (rightmost) bin includes underflow (overflow).

2016 and 2017 data-taking periods were affected by an erroneous “prefiring” of the L1 trigger on the previous bunch crossing, prohibiting the triggering of some fraction of potential signal events. We evaluate the resulting uncertainty in the trigger efficiency using a preliminary L1 prefiring efficiency map based on the end of the 2017 data-taking period, representing a worst case scenario.

- *dE/dx calibration*: A time-dependent calibration of the dE/dx measurement is performed using tracks associated with a muon, with the dE/dx value extracted from a Gaussian fit around the peak of the dE/dx distribution. A similar set of calibration factors is derived using low- p_T protons from Λ baryon decays. The difference in the calibration factors derived from the muons and protons is used to determine a systematic uncertainty in the dE/dx calibration.

The following systematic uncertainties are evaluated for the estimates of the number of background events.

- *Spurious-particle contamination*: An uncertainty of 100% is assigned to the estimated number of genuine-particle short-track background events to account for the pres-

Table 7: Upper: The considered sources of systematic uncertainty in the predicted signal yield and the corresponding range of values over the 49 search regions. A value of 0 is reported when the relative uncertainty is determined to be less than 0.5%. Lower: The ranges for the total pre-fit uncertainty in the predicted background counts with respect to the respective background contribution.

Uncertainty source	Relative uncertainty in yield (%)
Signal	
Dtk selection efficiency	10–17
Integrated luminosity	1.6
Jet energy scale and resolution	0–24
b jet tagging	0–4
Renormalization and factorization scales	0–2
Initial-state radiation	0–3
Pileup modeling	0–2
Trigger efficiency	0–4
dE/dx calibration	3–8
Background	
Genuine particle showering long	20–28
Genuine particle showering short	100–104
Genuine particle muon long	25–38
Spurious particle long	5–52
Spurious particle short	6–28

ence of spurious-particle contamination in the DY CR used to calculate the $\kappa_{\text{high}}^{\text{low}}$ transfer factors for this category. A 100% uncertainty is assigned because the measurement region for short tracks is dominated by spurious tracks and, after the subtraction, this is the order of how well the transfer factor is known. This uncertainty does not impact the sensitivity because this background is nearly negligible in the short track SRs.

- *Residual p_T dependence:* Differences in the predicted and observed p_T spectra of DTks in the transfer factor CRs are used to assess uncertainties of 30 and 20% in the number of spurious-particle long-track and genuine-particle long-track background events, respectively.

Statistical uncertainties in the SRs and CRs are accounted for in the fit described in Section 10.

The sources of systematic uncertainty and their assessed ranges across the 49 SRs are summarized in Table 7.

10 Results and interpretation

Figures 7 and 8 show a comparison in the baseline region between the data and pre-fit background prediction for the N_{jet} , $N_{\text{b-jet}}$, $p_{\text{T,hard}}^{\text{miss}}$, N_e , N_{μ} , and $m_{\text{DTk};dE/dx}$ distributions. The results for long tracks are shown in Fig. 7 and for short tracks in Fig. 8. Figure 9 presents the pre-fit (left) and post-fit (right) background predictions in comparison to the data in the 49 individual SRs. The corresponding numerical results for the pre-fit predictions are given in Table 8. For purposes of illustration, these figures and table include example results for the T6tbLL and T5btbLL models, with choices for squark (or gluino) mass, LSP mass, and chargino $c\tau$

value as indicated in the legends or table header. The data are found to be consistent with the background-only hypothesis, and therefore no evidence for new physics is observed. A slight systematic over-prediction is seen in the short-track category, consistent with the presence of spurious-particle contamination in the showering background sidebands. The background uncertainty model accounts for this effect via a nuisance parameter that reduces the total genuine-particle background yield for short track bins to nearly zero.

Upper limits on the production cross sections of the considered simplified models are computed using a maximum likelihood fit. The likelihood is a product of Poisson functions, one for each SR, accounting for the expected yields and evaluated using the observed event counts. The mean expected background and signal yields are constrained using gamma functions that account for the observed event counts in each sideband control region and for the simulated signal event counts. Other sources of uncertainty are accounted for using log-normal functions, with one nuisance parameter per source of uncertainty. Limits are determined under the asymptotic approximation [102] of the CL_s criterion described in Refs. [103, 104]. All 49 SRs are used in evaluating the limits for each signal model point. For the models of gluino pair production and top or bottom squark pair production, limits are derived in the mass plane of the mother particle and the LSP for different choices of chargino $c\tau$. We evaluate 95% confidence level (CL) upper limits on the signal cross sections. The approximate NNLO+NNLL cross section is used to determine corresponding mass exclusion curves. Expected limits are computed using the background-only hypothesis in place of the observed numbers of events.

For the strong production models, the sensitivity of our results depends on the mass difference $\Delta m_{(\tilde{g}, \tilde{q})-\text{LSP}}$ between the gluino or squark and the LSP. The limits weaken when $\Delta m_{(\tilde{g}, \tilde{q})-\text{LSP}}$ is small because of the resulting small boost (and thus short decay length) of the chargino in the detector frame. The limits also weaken for small LSP masses because of the significant boost of the chargino, which increasingly fails to decay within the tracker volume as $\Delta m_{(\tilde{g}, \tilde{q})-\text{LSP}}$ increases. The strongest constraints on the cross section reside at varying intermediate values of $\Delta m_{(\tilde{g}, \tilde{q})-\text{LSP}}$, depending on the chargino $c\tau$.

Upper limits on the cross section for the T6tbLL and T6btLL models are presented in Fig. 10. For the T6tbLL model, we exclude bottom squarks below a mass of 900–1540 GeV, depending on the LSP mass and chargino lifetime. Charginos and LSPs, taken to be essentially mass degenerate in our study, are excluded up to a mass of 850 (1210) GeV for chargino $c\tau = 10$ (200) cm, depending on the bottom squark mass. The analogous limits for the T6btLL model are 1100–1590 GeV for the top squark mass, and 1050 (1400) GeV for the chargino and LSP mass. These results extend the maximum limit on the LSP mass in the compressed phase space scenario by hundreds of GeV compared to the previous study [22], both for $c\tau = 10$ and 200 cm.

Upper limits on the cross section for the T5btbtLL model are presented in Fig. 11. Gluinos are excluded below a mass of 1450–2300 GeV, depending on LSP mass and chargino lifetime. Charginos and LSPs are excluded up to a maximum of 1950 GeV, depending on the gluino mass and chargino lifetime.

In Figs. 10 and 11, the white bands indicate the regions previously excluded by the CERN LEP (Large Electron-Positron Collider) experiments [105].

We examined the change in sensitivity introduced by our inclusion of the electron+DTk and muon+DTk channels in the analysis. We find that, compared to using the fully hadronic channel alone, addition of these channels leads to an improvement of around 40 GeV in the top squark mass limit and of around 100 GeV in both the bottom squark and gluino mass limits.

Finally, limits on pure wino [29] and higgsino [32] DM models are presented in Fig. 12 for

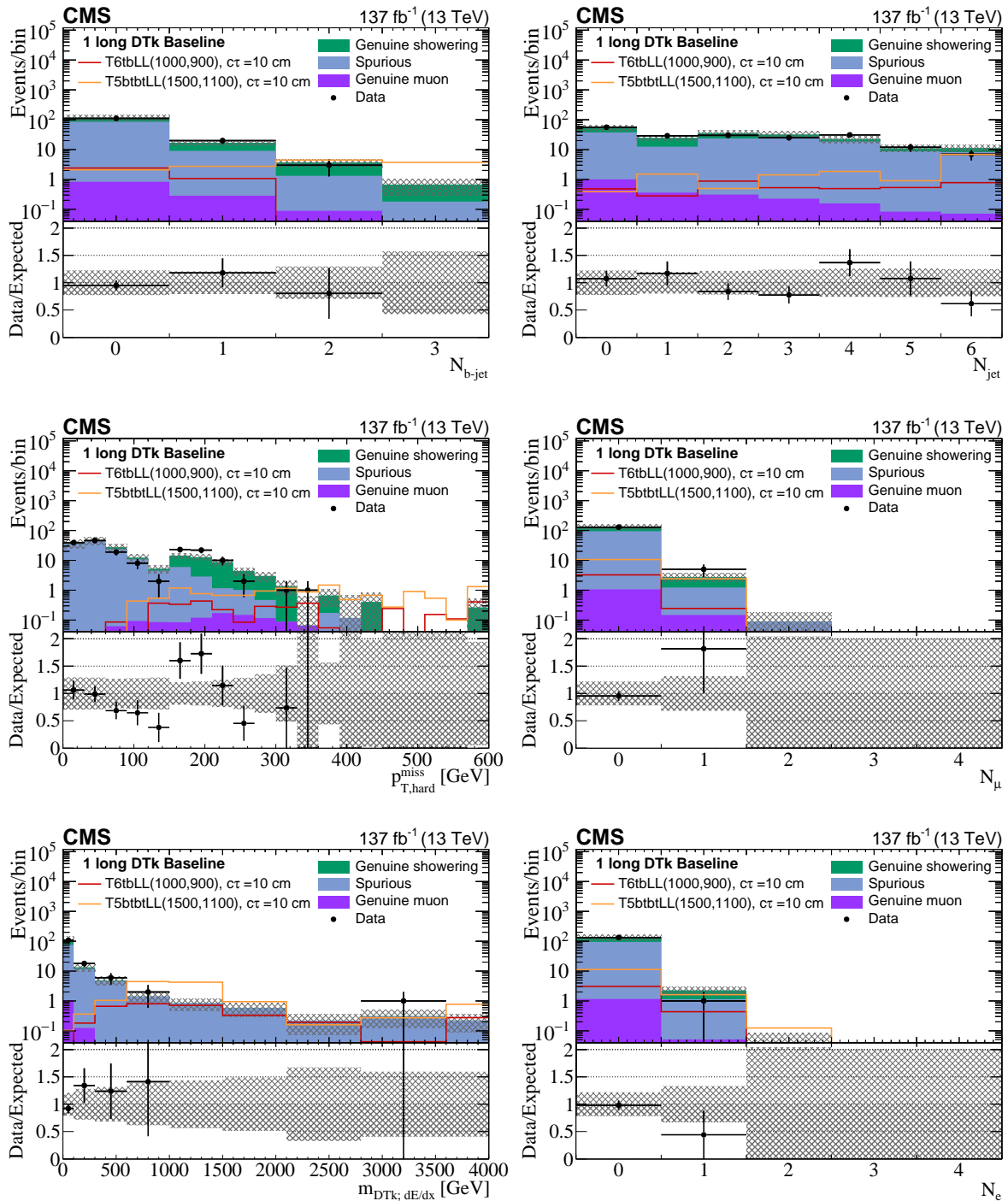


Figure 7: Comparison in the baseline region for the long-track DTK category between the data and pre-fit predicted SM background for the N_{jet} (upper left), $N_{\text{b-jet}}$ (upper right), $p_{\text{T,hard}}^{\text{miss}}$ (middle left), N_e (middle right), N_μ (lower left), and $m_{\text{DTk};dE/dx}$ (lower right) distributions. The uncertainty bars on the ratios in the lower panels indicate the fractional Poisson uncertainties in the observed counts. The gray bands show the fractional Poisson uncertainties in the control region counts, added in quadrature with the systematic uncertainties. The leftmost (rightmost) bin includes underflow (overflow). For purposes of illustration, results from the T6tbLL and T5btbtLL models are shown, where the first and second numbers in parentheses indicate the squark (or gluino) mass and the LSP mass, respectively, in GeV.

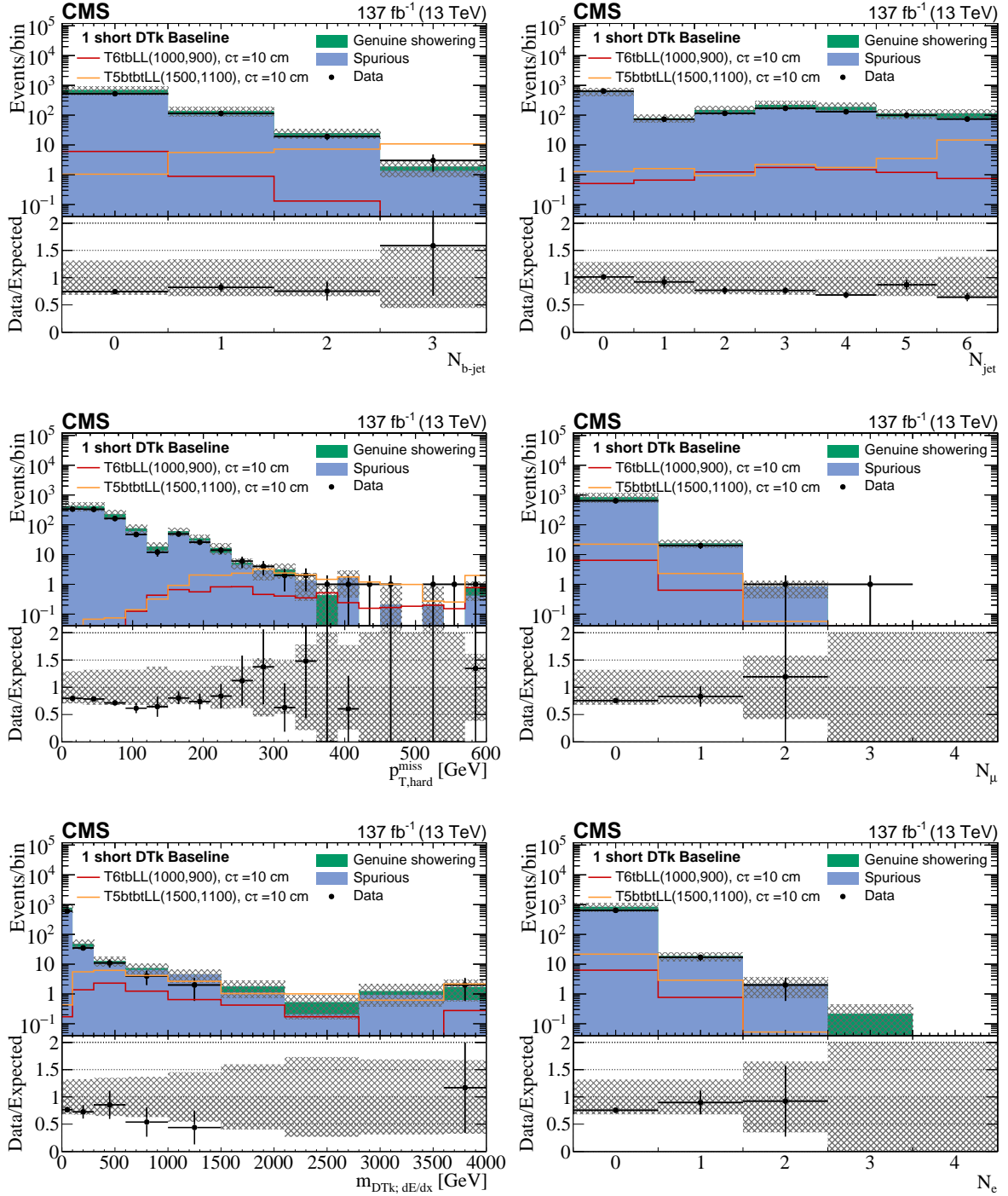


Figure 8: Comparison in the baseline region for the short-track DTK category between the data and pre-fit predicted SM background for the N_{jet} (upper left), $N_{\text{b-jet}}$ (upper right), $p_{\text{T,hard}}^{\text{miss}}$ (middle left), N_e (middle right), N_{μ} (lower left), and $m_{\text{DTk};dE/dx}$ (lower right) distributions. The uncertainty bars on the ratios in the lower panels indicate the fractional Poisson uncertainties in the observed counts. The gray bands show the fractional Poisson uncertainties in the control region counts, added in quadrature with the systematic uncertainties. The leftmost (rightmost) bin includes underflow (overflow). For purposes of illustration, results from the T6tbLL and T5btbtLL models are shown, where the first and second numbers in parentheses indicate the squark (or gluino) mass and the LSP mass, respectively, in GeV.

Table 8: Predicted pre-fit background and uncertainties in the 49 search regions (SRs). Statistical and bin-wise systematic uncertainties are added in quadrature. The control region (CR) counts corresponding to each background category are given in the column to the left of the respective column. The numbers in parentheses for the signal points indicate the squark (or gluino) mass in GeV, the LSP mass in GeV, and $c\tau$ for the chargino in cm, respectively.

SR number	CR	Spurious	CR	Showering	CR	Muon	Total bkg.	T6tbLL (1000, 900, 200)	T5btbtLL (1500, 1100, 10)	Observed
1	80	6.40 ± 0.72	56	17.2 ± 2.3	313	0.23 ± 0.01	23.9 ± 2.4	0.10 ± 0.06	0.00 ± 0.00	33
2	14	1.12 ± 0.30	4	1.23 ± 0.61	17	0.01 ± 0.01	2.36 ± 0.68	0.80 ± 0.17	0.00 ± 0.00	3
3	170	58.9 ± 4.5	33	8.1 ± 1.4	0	0.00 ± 0.00	67.0 ± 4.7	0.04 ± 0.03	0.00 ± 0.00	51
4	23	8.0 ± 1.7	3	0.74 ± 0.43	0	0.00 ± 0.00	8.7 ± 1.7	0.17 ± 0.07	0.00 ± 0.00	5
5	44	3.52 ± 0.53	24	7.4 ± 1.5	183	0.13 ± 0.01	11.0 ± 1.6	0.77 ± 0.16	0.03 ± 0.03	10
6	7	0.56 ± 0.21	1	0.31 ± 0.31	9	0.01 ± 0.01	0.87 ± 0.37	4.86 ± 0.38	0.00 ± 0.00	1
7	92	31.9 ± 3.3	23	5.7 ± 1.2	0	0.00 ± 0.00	37.5 ± 3.5	0.19 ± 0.07	0.00 ± 0.00	25
8	10	3.5 ± 1.1	2	0.49 ± 0.35	0	0.00 ± 0.00	4.0 ± 1.2	1.02 ± 0.15	0.03 ± 0.02	1
9	4	0.32 ± 0.16	8	2.46 ± 0.87	37	0.03 ± 0.03	2.81 ± 0.88	0.00 ± 0.00	0.00 ± 0.00	3
10	1	0.08 ± 0.08	0	$0.00^{+0.57}_{-0.00}$	0	0.00 ± 0.00	$0.08^{+0.57}_{-0.08}$	0.06 ± 0.04	0.00 ± 0.00	0
11	10	3.5 ± 1.1	4	0.98 ± 0.49	0	0.00 ± 0.00	4.5 ± 1.2	0.00 ± 0.00	0.00 ± 0.00	4
12	2	0.69 ± 0.49	0	$0.00^{+0.90}_{-0.00}$	0	0.00 ± 0.00	$0.7^{+1.0}_{-0.7}$	0.00 ± 0.00	0.11 ± 0.11	0
13	10	0.80 ± 0.25	15	4.6 ± 1.2	157	0.12 ± 0.01	5.5 ± 1.2	0.14 ± 0.07	0.18 ± 0.10	7
14	1	0.08 ± 0.08	0	$0.00^{+0.57}_{-0.00}$	5	0.00 ± 0.00	$0.08^{+0.57}_{-0.08}$	1.19 ± 0.18	0.96 ± 0.27	0
15	31	10.7 ± 1.9	12	2.95 ± 0.85	0	0.00 ± 0.00	13.7 ± 2.1	0.03 ± 0.02	0.61 ± 0.17	9
16	5	1.73 ± 0.77	0	$0.00^{+0.90}_{-0.00}$	0	0.00 ± 0.00	1.7 ± 1.2	0.18 ± 0.06	3.41 ± 0.42	3
17	1	0.08 ± 0.08	4	1.23 ± 0.61	186	0.14 ± 0.01	1.45 ± 0.62	0.07 ± 0.05	0.00 ± 0.00	0
18	0	0.01 ± 0.01	0	$0.00^{+0.57}_{-0.00}$	12	0.01 ± 0.01	$0.02^{+0.57}_{-0.02}$	0.67 ± 0.18	0.00 ± 0.00	0
19	7	2.42 ± 0.92	2	0.49 ± 0.35	0	0.00 ± 0.00	2.92 ± 0.98	0.00 ± 0.00	0.00 ± 0.00	4
20	3	1.04 ± 0.60	1	0.25 ± 0.25	0	0.00 ± 0.00	1.28 ± 0.65	0.07 ± 0.04	0.00 ± 0.00	1
21	2	0.16 ± 0.11	4	1.23 ± 0.61	198	0.15 ± 0.01	1.54 ± 0.63	0.61 ± 0.14	1.19 ± 0.35	2
22	0	0.03 ± 0.03	0	$0.00^{+0.57}_{-0.00}$	10	0.01 ± 0.01	$0.04^{+0.57}_{-0.04}$	4.81 ± 0.40	1.91 ± 0.40	0
23	9	3.1 ± 1.0	5	1.23 ± 0.55	0	0.00 ± 0.00	4.4 ± 1.2	0.10 ± 0.05	0.94 ± 0.16	6
24	1	0.35 ± 0.35	0	$0.00^{+0.90}_{-0.00}$	0	0.00 ± 0.00	$0.35^{+0.97}_{-0.35}$	1.22 ± 0.19	4.10 ± 0.51	0
25	6	0.48 ± 0.20	1	0.31 ± 0.31	23	0.02 ± 0.02	0.80 ± 0.36	0.02 ± 0.02	0.09 ± 0.09	3
26	4	0.32 ± 0.16	0	$0.00^{+0.57}_{-0.00}$	1	0.00 ± 0.00	$0.32^{+0.59}_{-0.32}$	0.08 ± 0.05	0.00 ± 0.00	0
27	42	14.6 ± 2.2	4	0.98 ± 0.49	0	0.00 ± 0.00	15.5 ± 2.3	0.00 ± 0.00	0.00 ± 0.00	13
28	8	2.77 ± 0.98	1	0.25 ± 0.25	0	0.00 ± 0.00	3.0 ± 1.0	0.02 ± 0.02	0.03 ± 0.03	2
29	3	0.24 ± 0.14	0	$0.00^{+0.57}_{-0.00}$	19	0.01 ± 0.01	$0.25^{+0.58}_{-0.25}$	0.00 ± 0.00	0.00 ± 0.00	0
30	3	0.24 ± 0.14	0	$0.00^{+0.57}_{-0.00}$	0	0.00 ± 0.00	$0.24^{+0.58}_{-0.24}$	0.00 ± 0.00	0.00 ± 0.00	0
31	8	2.77 ± 0.98	1	0.25 ± 0.25	0	0.00 ± 0.00	3.0 ± 1.0	0.00 ± 0.00	0.00 ± 0.00	2
32	3	1.04 ± 0.60	0	$0.00^{+0.90}_{-0.00}$	0	0.00 ± 0.00	$1.0^{+1.1}_{-1.0}$	0.00 ± 0.00	0.03 ± 0.02	0
33	3	0.24 ± 0.14	4	1.23 ± 0.61	155	0.11 ± 0.01	1.58 ± 0.63	0.06 ± 0.04	0.48 ± 0.25	2
34	0	0.04 ± 0.04	0	$0.00^{+0.57}_{-0.00}$	6	0.00 ± 0.00	$0.05^{+0.57}_{-0.05}$	0.71 ± 0.16	0.59 ± 0.27	0
35	20	6.9 ± 1.6	2	0.49 ± 0.35	0	0.00 ± 0.00	7.4 ± 1.6	0.00 ± 0.00	0.31 ± 0.18	4
36	2	0.69 ± 0.49	1	0.25 ± 0.25	0	0.00 ± 0.00	0.94 ± 0.55	0.12 ± 0.06	0.76 ± 0.22	1
37	9	0.72 ± 0.24	0	$0.00^{+0.57}_{-0.00}$	7	0.01 ± 0.01	0.73 ± 0.61	0.03 ± 0.03	0.00 ± 0.00	0
38	3	0.24 ± 0.14	0	$0.00^{+0.57}_{-0.00}$	1	0.00 ± 0.00	$0.24^{+0.58}_{-0.24}$	0.04 ± 0.04	0.01 ± 0.01	1
39	39	13.5 ± 2.2	5	1.23 ± 0.55	0	0.00 ± 0.00	14.7 ± 2.2	0.00 ± 0.00	0.00 ± 0.00	10
40	2	0.69 ± 0.49	1	0.25 ± 0.25	0	0.00 ± 0.00	0.94 ± 0.55	0.00 ± 0.00	0.00 ± 0.00	2
41	1	0.08 ± 0.08	1	0.31 ± 0.31	12	0.01 ± 0.01	0.40 ± 0.32	0.00 ± 0.00	0.00 ± 0.00	0
42	0	0.01 ± 0.01	0	$0.00^{+0.57}_{-0.00}$	0	0.00 ± 0.00	$0.01^{+0.57}_{-0.01}$	0.00 ± 0.00	0.00 ± 0.00	0
43	6	2.08 ± 0.85	3	0.74 ± 0.43	0	0.00 ± 0.00	2.82 ± 0.95	0.00 ± 0.00	0.00 ± 0.00	4
44	0	0.37 ± 0.37	0	$0.00^{+0.90}_{-0.00}$	0	0.00 ± 0.00	$0.37^{+0.98}_{-0.37}$	0.00 ± 0.00	0.03 ± 0.02	0
45	5	0.40 ± 0.18	3	0.92 ± 0.53	47	0.03 ± 0.01	1.36 ± 0.56	0.27 ± 0.10	0.14 ± 0.05	0
46	0	0.07 ± 0.07	0	$0.00^{+0.57}_{-0.00}$	3	0.00 ± 0.00	$0.07^{+0.57}_{-0.07}$	1.12 ± 0.22	0.72 ± 0.22	0
47	13	4.5 ± 1.3	2	0.49 ± 0.35	0	0.00 ± 0.00	5.0 ± 1.3	0.00 ± 0.00	0.37 ± 0.14	3
48	2	0.69 ± 0.49	0	$0.00^{+0.90}_{-0.00}$	0	0.00 ± 0.00	$0.7^{+1.0}_{-0.7}$	0.27 ± 0.09	0.91 ± 0.19	0
49	1	0.35 ± 0.35	0	$0.00^{+0.57}_{-0.00}$	1	0.00 ± 0.00	$0.35^{+0.66}_{-0.35}$	4.57 ± 0.39	0.66 ± 0.24	0

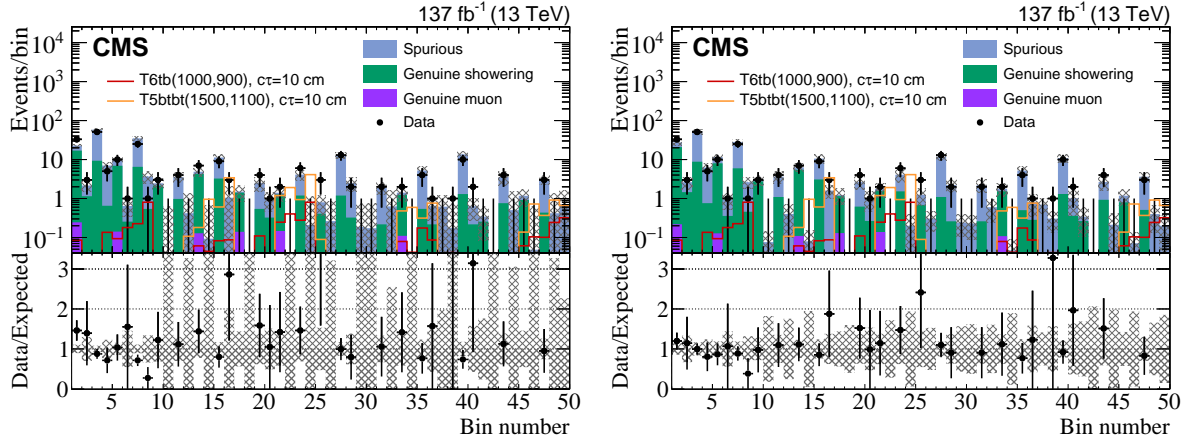


Figure 9: Comparison between the data and SM background predictions for the 49 search regions. The left (right) plot shows the pre-fit (post-fit) background predictions. The uncertainty bars on the ratios in the lower panels, shown for bins with nonzero entries, indicate the fractional Poisson uncertainties in the observed counts. The gray bands show the fractional Poisson uncertainties in the control region counts, added in quadrature with the systematic uncertainties. For purposes of illustration, results from the T6tbLL and T5btbtLL models are shown, where the first and second numbers in parentheses indicate the squark (or gluino) mass and the LSP mass, respectively, in GeV.

the case of a minimal mass splitting Δm^\pm between the two lightest SUSY states, bounded by two-loop radiative corrections. The chargino lifetime is determined as a function of Δm^\pm , as described in Ref. [30] for the wino case and in Ref. [31] for the higgsino case. The production scenario accounts for the TChiWZ, TChiWW, and TChiW models taken together, where the first process occurs only in the higgsino case. The green line indicates the minimum mass splitting required by the radiative corrections. Chargino and LSP masses are excluded up to 650 GeV for the pure wino model and up to 190 GeV for the pure higgsino model.

11 Summary

A search for long-lived charginos based on data collected in proton-proton collisions at $\sqrt{s} = 13$ TeV, corresponding to an integrated luminosity of 137 fb^{-1} , is presented. Event yields are studied in 49 nonoverlapping search regions defined by the number of electrons, muons, jets, and b-tagged jets, and by the hard missing transverse momentum, in final states with at least one identified disappearing track. Further categorization of the SRs is based on the approximate length of the track and on its dE/dx energy loss in the inner tracking detector. The analysis targets a wide variety of possible production modes appearing in simplified models of R -parity conserving supersymmetry, including gluino, top squark, bottom squark, and electroweakino pair production. A machine-learning-based classifier is employed to optimally select disappearing tracks, while rejecting tracks originating from failures in the reconstruction or from combinatorial effects. Background contributions to the SRs are evaluated based on the observed yields in data control regions. The observed yields in the SRs are found to be consistent with the background-only predictions, and thus no evidence for supersymmetry is found.

In the context of the examined models, bottom squarks, top squarks, and gluinos with masses as large as 1540, 1590, and 2300 GeV, respectively, are excluded. For bottom squark pair pro-

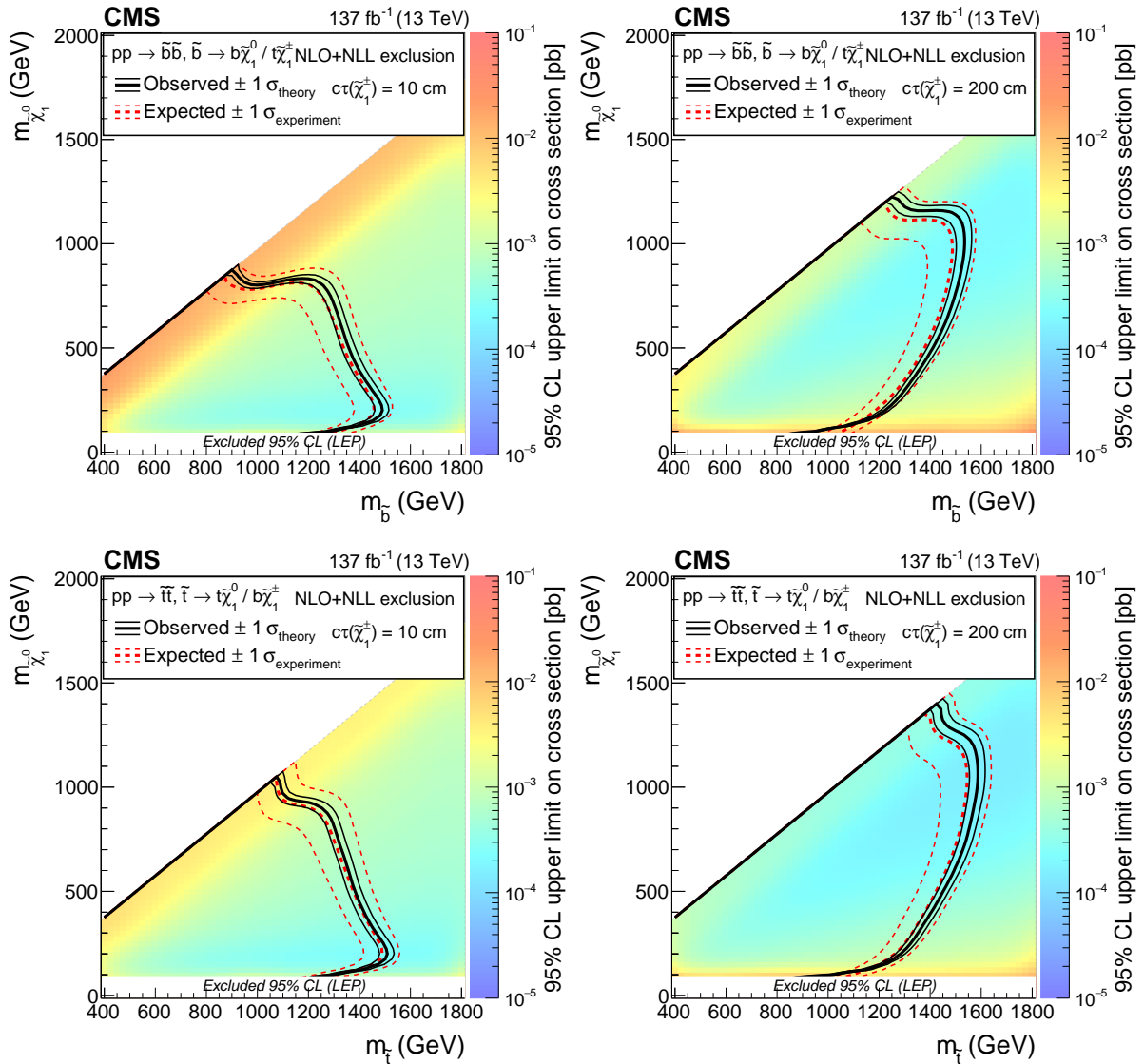


Figure 10: Observed 95% CL upper limits on the signal cross sections (colored area) versus the bottom or top squark and neutralino mass for the T6tbLL (upper) and T6btLL (lower) model for a chargino proper decay length $c\tau$ of 10 (left column) or 200 (right column) cm. Also shown are black (red) contours corresponding to the observed (expected) lower limits, including their uncertainties, on the squark and neutralino masses.

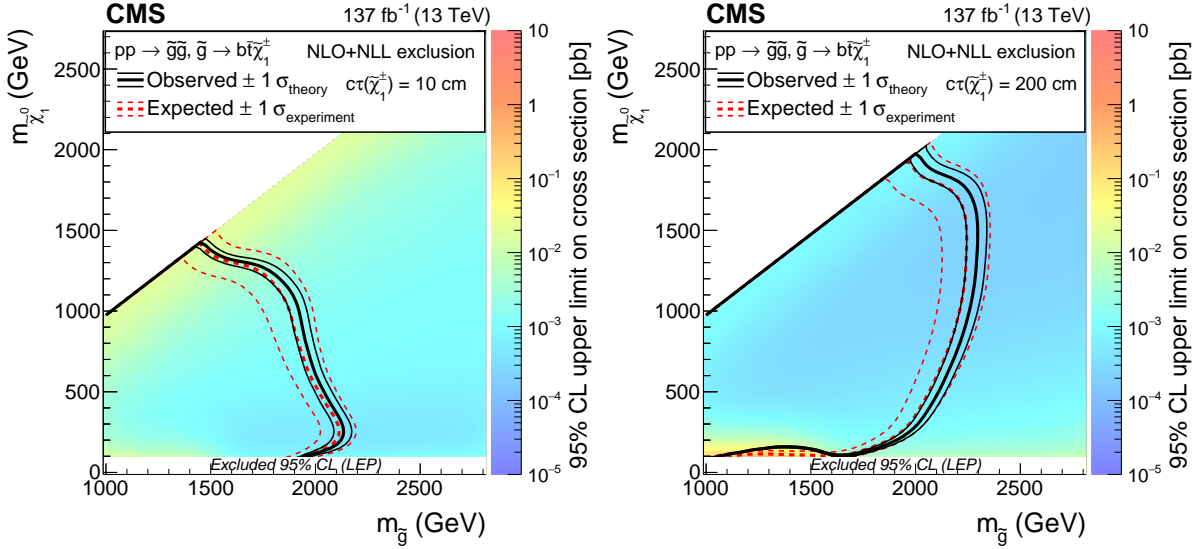


Figure 11: Observed 95% CL upper limits on the signal cross sections (colored area) versus the gluino and neutralino mass for the T5btbtLL model for a chargino proper decay length $c\tau$ of 10 (left column) and 200 (right column) cm. Also shown are black (red) contours corresponding to the observed (expected) lower limits, including their uncertainties, on the gluino and neutralino masses.

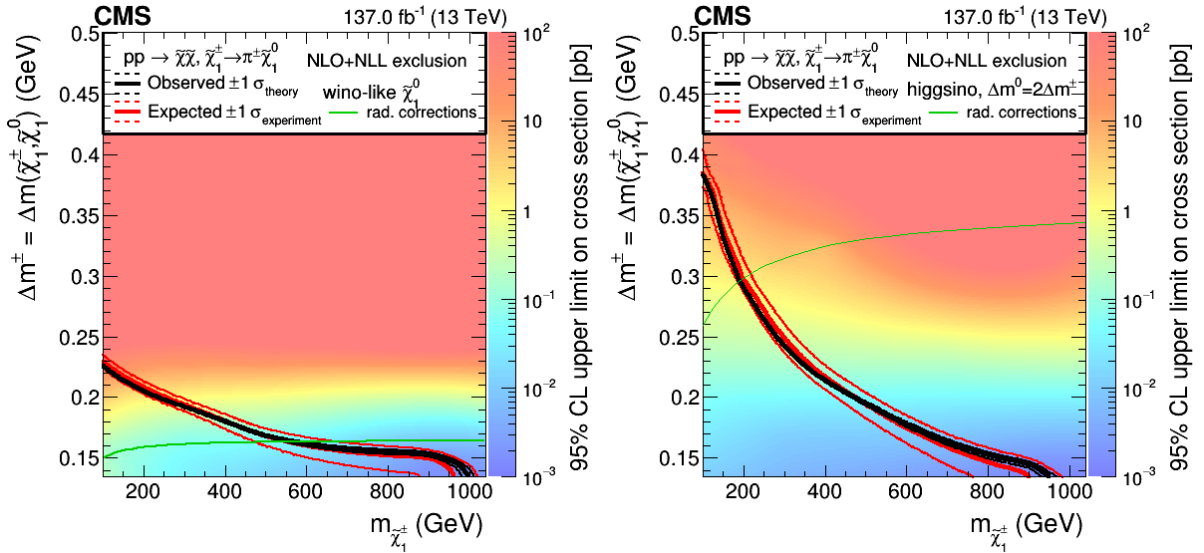


Figure 12: Observed 95% CL upper limits on the signal cross sections (colored area) versus the chargino-LSP mass difference and the mass of the chargino for the wino (left) and higgsino (right) DM models. The black contours indicate the boundary where the observed upper limit equals the cross section of fully degenerate electroweakino production. The corresponding expected limits are shown by the red contours. The green lines represent the set of model points corresponding to the pure wino and pure higgsino models where only radiative corrections to the mass splitting are assumed. Chargino lifetimes are based on two-loop calculations.

duction, charginos and the lightest supersymmetric particle, considered to be essentially mass degenerate in our study, are excluded up to a mass of 850 (1210) GeV for a chargino proper decay length $c\tau$ of 10 (200) cm. For top squark pair production, the corresponding limit on the chargino and LSP mass is 1050 (1400) GeV. These results extend the maximum limit on the LSP mass in the compressed phase space scenario by hundreds of GeV compared to the previous study [22], and extend the reach of sensitivity into mass regions where a pure wino- or pure higgsino-like LSP can account for the observed dark matter relic density. Limits are also determined for a pure wino dark matter model [29] and a pure higgsino dark matter model [32]. In the context of these two models, charginos and LSPs are excluded up to 650 GeV for the wino model and up to 190 GeV for the higgsino model.

Acknowledgments

We congratulate our colleagues in the CERN accelerator departments for the excellent performance of the LHC and thank the technical and administrative staffs at CERN and at other CMS institutes for their contributions to the success of the CMS effort. In addition, we gratefully acknowledge the computing centers and personnel of the Worldwide LHC Computing Grid and other centers for delivering so effectively the computing infrastructure essential to our analyses. Finally, we acknowledge the enduring support for the construction and operation of the LHC, the CMS detector, and the supporting computing infrastructure provided by the following funding agencies: SC (Armenia); BMBWF and FWF (Austria); FNRS and FWO (Belgium); CNPq, CAPES, FAPERJ, FAPERGS, and FAPESP (Brazil); MES and BNSF (Bulgaria); CERN; CAS, MoST, and NSFC (China); MINCIENCIAS (Colombia); MSES and CSF (Croatia); RIF (Cyprus); SENESCYT (Ecuador); MoER, ERC PUT and ERDF (Estonia); Academy of Finland, MEC, and HIP (Finland); CEA and CNRS/IN2P3 (France); SRNSF (Georgia); BMBF, DFG, and HGF (Germany); GSRI (Greece); NKFIH (Hungary); DAE and DST (India); IPM (Iran); SFI (Ireland); INFN (Italy); MSIP and NRF (Republic of Korea); MES (Latvia); LAS (Lithuania); MOE and UM (Malaysia); BUAP, CINVESTAV, CONACYT, LNS, SEP, and UASLP-FAI (Mexico); MOS (Montenegro); MBIE (New Zealand); PAEC (Pakistan); MES and NSC (Poland); FCT (Portugal); MESTD (Serbia); MCIN/AEI and PCTI (Spain); MOSTR (Sri Lanka); Swiss Funding Agencies (Switzerland); MST (Taipei); MHESI and NSTDA (Thailand); TUBITAK and TEN-MAK (Turkey); NASU (Ukraine); STFC (United Kingdom); DOE and NSF (USA).

Individuals have received support from the Marie-Curie program and the European Research Council and Horizon 2020 Grant, contract Nos. 675440, 724704, 752730, 758316, 765710, 824093, and COST Action CA16108 (European Union); the Leventis Foundation; the Alfred P. Sloan Foundation; the Alexander von Humboldt Foundation; the Science Committee, project no. 22rl-037 (Armenia); the Belgian Federal Science Policy Office; the Fonds pour la Formation à la Recherche dans l'Industrie et dans l'Agriculture (FRIA-Belgium); the Agentschap voor Innovatie door Wetenschap en Technologie (IWT-Belgium); the F.R.S.-FNRS and FWO (Belgium) under the "Excellence of Science – EOS" – be.h project n. 30820817; the Beijing Municipal Science & Technology Commission, No. Z191100007219010 and Fundamental Research Funds for the Central Universities (China); the Ministry of Education, Youth and Sports (MEYS) of the Czech Republic; the Shota Rustaveli National Science Foundation, grant FR-22-985 (Georgia); the Deutsche Forschungsgemeinschaft (DFG), under Germany's Excellence Strategy – EXC 2121 "Quantum Universe" – 390833306, and under project number 400140256 - GRK2497; the Hellenic Foundation for Research and Innovation (HFRI), Project Number 2288 (Greece); the Hungarian Academy of Sciences, the New National Excellence Program - ÚNKP, the NKFIH research grants K 124845, K 124850, K 128713, K 128786, K 129058, K 131991, K 133046, K 138136, K 143460, K 143477, 2020-2.2.1-ED-2021-00181, and TKP2021-NKTA-64 (Hungary); the Council

of Science and Industrial Research, India; the Latvian Council of Science; the Ministry of Education and Science, project no. 2022/WK/14, and the National Science Center, contracts Opus 2021/41/B/ST2/01369 and 2021/43/B/ST2/01552 (Poland); the Fundação para a Ciência e a Tecnologia, grant CEECIND/01334/2018 (Portugal); the National Priorities Research Program by Qatar National Research Fund; MCIN/AEI/10.13039/501100011033, ERDF “a way of making Europe,” and the Programa Estatal de Fomento de la Investigación Científica y Técnica de Excelencia María de Maeztu, grant MDM-2017-0765 and Programa Severo Ochoa del Principado de Asturias (Spain); the Chulalongkorn Academic into Its 2nd Century Project Advancement Project, and the National Science, Research and Innovation Fund via the Program Management Unit for Human Resources & Institutional Development, Research and Innovation, grant B05F650021 (Thailand); the Kavli Foundation; the Nvidia Corporation; the SuperMicro Corporation; the Welch Foundation, contract C-1845; and the Weston Havens Foundation (USA).

References

- [1] P. Ramond, “Dual theory for free fermions”, *Phys. Rev. D* **3** (1971) 2415, doi:10.1103/PhysRevD.3.2415.
- [2] Y. A. Gol’fand and E. P. Likhtman, “Extension of the algebra of Poincaré group generators and violation of P invariance”, *JETP Lett.* **13** (1971) 323.
- [3] A. Neveu and J. H. Schwarz, “Factorizable dual model of pions”, *Nucl. Phys. B* **31** (1971) 86, doi:10.1016/0550-3213(71)90448-2.
- [4] D. V. Volkov and V. P. Akulov, “Possible universal neutrino interaction”, *JETP Lett.* **16** (1972) 438.
- [5] J. Wess and B. Zumino, “A Lagrangian model invariant under supergauge transformations”, *Phys. Lett. B* **49** (1974) 52, doi:10.1016/0370-2693(74)90578-4.
- [6] J. Wess and B. Zumino, “Supergauge transformations in four dimensions”, *Nucl. Phys. B* **70** (1974) 39, doi:10.1016/0550-3213(74)90355-1.
- [7] P. Fayet, “Supergauge invariant extension of the Higgs mechanism and a model for the electron and its neutrino”, *Nucl. Phys. B* **90** (1975) 104, doi:10.1016/0550-3213(75)90636-7.
- [8] P. Fayet and S. Ferrara, “Supersymmetry”, *Phys. Rept.* **32** (1977) 249, doi:10.1016/0370-1573(77)90066-7.
- [9] H. P. Nilles, “Supersymmetry, supergravity and particle physics”, *Phys. Rep.* **110** (1984) 1, doi:10.1016/0370-1573(84)90008-5.
- [10] F. Zwicky, “On the masses of nebulae and of clusters of nebulae”, *Astrophys. J.* **86** (1937) 217, doi:10.1086/143864.
- [11] V. C. Rubin and W. K. Ford, Jr., “Rotation of the Andromeda nebula from a spectroscopic survey of emission regions”, *Astrophys. J.* **159** (1970) 379, doi:10.1086/150317.
- [12] L. Susskind, “Dynamics of spontaneous symmetry breaking in the Weinberg-Salam theory”, *Phys. Rev. D* **20** (1979) 2619, doi:10.1103/PhysRevD.20.2619.

- [13] G. 't Hooft, "Naturalness, chiral symmetry, and spontaneous chiral symmetry breaking", *NATO Sci. Ser. B* **59** (1980) 135, doi:10.1007/978-1-4684-7571-5_9.
- [14] M. J. G. Veltman, "The infrared-ultraviolet connection", *Acta Phys. Polon. B* **12** (1981) 437.
- [15] ATLAS Collaboration, "The ATLAS experiment at the CERN Large Hadron Collider", *JINST* **3** (2008) S08003, doi:10.1088/1748-0221/3/08/S08003.
- [16] CMS Collaboration, "The CMS experiment at the CERN LHC", *JINST* **3** (2008) S08004, doi:10.1088/1748-0221/3/08/S08004.
- [17] Planck Collaboration, "Planck 2018 results. VI. Cosmological parameters", *Astron. Astrophys.* **641** (2020) A6, doi:10.1051/0004-6361/201833910, arXiv:1807.06209. [Erratum: doi:10.1051/0004-6361/201833910e].
- [18] G. R. Farrar and P. Fayet, "Phenomenology of the production, decay, and detection of new hadronic states associated with supersymmetry", *Phys. Lett. B* **76** (1978) 575, doi:10.1016/0370-2693(78)90858-4.
- [19] A. Delgado and M. Quirós, "Higgsino dark matter in the MSSM", *Phys. Rev. D* **103** (2021) 015024, doi:10.1103/PhysRevD.103.015024, arXiv:2008.00954.
- [20] K. Griest and D. Seckel, "Three exceptions in the calculation of relic abundances", *Phys. Rev. D* **43** (1991) 3191, doi:10.1103/PhysRevD.43.3191.
- [21] G. Jungman, M. Kamionkowski, and K. Griest, "Supersymmetric dark matter", *Phys. Rept.* **267** (1996) 195, doi:10.1016/0370-1573(95)00058-5, arXiv:hep-ph/9506380.
- [22] CMS Collaboration, "Searches for physics beyond the standard model with the M_{T2} variable in hadronic final states with and without disappearing tracks in proton-proton collisions at $\sqrt{s} = 13$ TeV", *Eur. Phys. J. C* **80** (2020) 3, doi:10.1140/epjc/s10052-019-7493-x, arXiv:1909.03460.
- [23] CMS Collaboration, "Search for disappearing tracks in proton-proton collisions at $\sqrt{s} = 13$ TeV", *Phys. Lett. B* **806** (2020) 135502, doi:10.1016/j.physletb.2020.135502, arXiv:2004.05153.
- [24] ATLAS Collaboration, "Search for long-lived charginos based on a disappearing-track signature using 136 fb^{-1} of pp collisions at $\sqrt{s} = 13$ TeV with the ATLAS detector", *Eur. Phys. J. C* **82** (2022) 606, doi:10.1140/epjc/s10052-022-10489-5, arXiv:2201.02472.
- [25] HEPData record for this analysis, 2023. doi:10.17182/hepdata.144178.
- [26] J. Alwall, P. C. Schuster, and N. Toro, "Simplified models for a first characterization of new physics at the LHC", *Phys. Rev. D* **79** (2009) 075020, doi:10.1103/PhysRevD.79.075020, arXiv:0810.3921.
- [27] D. Alves et al., "Simplified models for LHC new physics searches", *J. Phys. G* **39** (2012) 105005, doi:10.1088/0954-3899/39/10/105005, arXiv:1105.2838.
- [28] CMS Collaboration, "Interpretation of searches for supersymmetry with simplified models", *Phys. Rev. D* **88** (2013) 052017, doi:10.1103/PhysRevD.88.052017, arXiv:1301.2175.

- [29] M. Ibe, S. Matsumoto, and R. Sato, “Mass splitting between charged and neutral winos at two-loop level”, *Phys. Lett. B* **721** (2013) 252, doi:10.1016/j.physletb.2013.03.015, arXiv:1212.5989.
- [30] M. Ibe, M. Mishima, Y. Nakayama, and S. Shirai, “Precise estimate of charged wino decay rate”, *JHEP* **01** (2023) 017, doi:10.1007/JHEP01(2023)017, arXiv:2210.16035.
- [31] N. Nagata and S. Shirai, “Higgsino dark matter in high-scale supersymmetry”, *JHEP* **01** (2015) 029, doi:10.1007/JHEP01(2015)029, arXiv:1410.4549.
- [32] H. Fukuda, N. Nagata, H. Otono, and S. Shirai, “Higgsino dark matter or not: role of disappearing track searches at the LHC and future colliders”, *Phys. Lett. B* **781** (2018) 306, doi:10.1016/j.physletb.2018.03.088, arXiv:1703.09675.
- [33] S. P. Martin, “A supersymmetry primer”, *Adv. Ser. Direct. High Energy Phys.* **18** (1998) 1, doi:10.1142/9789812839657_0001, arXiv:hep-ph/9709356.
- [34] B. C. Allanach, “SOFTSUSY: a program for calculating supersymmetric spectra”, *Comput. Phys. Commun.* **143** (2002) 305, doi:10.1016/S0010-4655(01)00460-X, arXiv:hep-ph/0104145.
- [35] CMS Tracker Group Collaboration, “The CMS phase-1 pixel detector upgrade”, *JINST* **16** (2021) P02027, doi:10.1088/1748-0221/16/02/P02027, arXiv:2012.14304.
- [36] CMS Collaboration, “The CMS trigger system”, *JINST* **12** (2017) P01020, doi:10.1088/1748-0221/12/01/P01020, arXiv:1609.02366.
- [37] CMS Collaboration, “Performance of the CMS Level-1 trigger in proton-proton collisions at $\sqrt{s} = 13$ TeV”, *JINST* **15** (2020) P10017, doi:10.1088/1748-0221/15/10/P10017, arXiv:2006.10165.
- [38] CMS Collaboration, “Particle-flow reconstruction and global event description with the CMS detector”, *JINST* **12** (2017) P10003, doi:10.1088/1748-0221/12/10/P10003, arXiv:1706.04965.
- [39] CMS Collaboration, “Electron and photon reconstruction and identification with the CMS experiment at the CERN LHC”, *JINST* **16** (2021) P05014, doi:10.1088/1748-0221/16/05/P05014, arXiv:2012.06888.
- [40] CMS Collaboration, “Performance of the CMS muon detector and muon reconstruction with proton-proton collisions at $\sqrt{s} = 13$ TeV”, *JINST* **13** (2018) P06015, doi:10.1088/1748-0221/13/06/P06015, arXiv:1804.04528.
- [41] CMS Collaboration, “Technical proposal for the Phase-II upgrade of the Compact Muon Solenoid”, CMS Technical Proposal CERN-LHCC-2015-010, CMS-TDR-15-02, 2015.
- [42] M. Cacciari, G. P. Salam, and G. Soyez, “The anti- k_T jet clustering algorithm”, *JHEP* **04** (2008) 063, doi:10.1088/1126-6708/2008/04/063, arXiv:0802.1189.
- [43] M. Cacciari, G. P. Salam, and G. Soyez, “FastJet user manual”, *Eur. Phys. J. C* **72** (2012) 1896, doi:10.1140/epjc/s10052-012-1896-2, arXiv:1111.6097.
- [44] CMS Collaboration, “Jet performance in pp collisions at $\sqrt{s} = 7$ TeV”, CMS Physics Analysis Summary CMS-PAS-JME-10-003, 2010.

- [45] CMS Collaboration, “Jet algorithms performance in 13 TeV data”, CMS Physics Analysis Summary CMS-PAS-JME-16-003, 2017.
- [46] CMS Collaboration, “Jet energy scale and resolution in the CMS experiment in pp collisions at 8 TeV”, *JINST* **12** (2017) P02014, doi:10.1088/1748-0221/12/02/P02014, arXiv:1607.03663.
- [47] M. Cacciari and G. P. Salam, “Pileup subtraction using jet areas”, *Phys. Lett. B* **659** (2008) 119, doi:10.1016/j.physletb.2007.09.077, arXiv:0707.1378.
- [48] CMS Collaboration, “Identification of heavy-flavour jets with the CMS detector in pp collisions at 13 TeV”, *JINST* **13** (2018) P05011, doi:10.1088/1748-0221/13/05/P05011, arXiv:1712.07158.
- [49] K. Rehermann and B. Tweedie, “Efficient identification of boosted semileptonic top quarks at the LHC”, *JHEP* **03** (2011) 059, doi:10.1007/JHEP03(2011)059, arXiv:1007.2221.
- [50] J. Alwall et al., “The automated computation of tree-level and next-to-leading order differential cross sections, and their matching to parton shower simulations”, *JHEP* **07** (2014) 079, doi:10.1007/JHEP07(2014)079, arXiv:1405.0301.
- [51] J. Alwall et al., “Comparative study of various algorithms for the merging of parton showers and matrix elements in hadronic collisions”, *Eur. Phys. J. C* **53** (2008) 473, doi:10.1140/epjc/s10052-007-0490-5, arXiv:0706.2569.
- [52] R. Frederix and S. Frixione, “Merging meets matching in MC@NLO”, *JHEP* **12** (2012) 061, doi:10.1007/JHEP12(2012)061, arXiv:1209.6215.
- [53] P. Nason, “A new method for combining NLO QCD with shower Monte Carlo algorithms”, *JHEP* **11** (2004) 040, doi:10.1088/1126-6708/2004/11/040, arXiv:hep-ph/0409146.
- [54] S. Frixione, P. Nason, and C. Oleari, “Matching NLO QCD computations with parton shower simulations: the POWHEG method”, *JHEP* **11** (2007) 070, doi:10.1088/1126-6708/2007/11/070, arXiv:0709.2092.
- [55] S. Alioli, P. Nason, C. Oleari, and E. Re, “A general framework for implementing NLO calculations in shower Monte Carlo programs: the POWHEG BOX”, *JHEP* **06** (2010) 043, doi:10.1007/JHEP06(2010)043, arXiv:1002.2581.
- [56] S. Alioli, P. Nason, C. Oleari, and E. Re, “NLO single-top production matched with shower in POWHEG: s - and t -channel contributions”, *JHEP* **09** (2009) 111, doi:10.1088/1126-6708/2009/09/111, arXiv:0907.4076. [Erratum: doi:10.1007/JHEP02(2010)011].
- [57] E. Re, “Single-top W_t -channel production matched with parton showers using the POWHEG method”, *Eur. Phys. J. C* **71** (2011) 1547, doi:10.1140/epjc/s10052-011-1547-z, arXiv:1009.2450.
- [58] T. Melia, P. Nason, R. Rontsch, and G. Zanderighi, “ W^+W^- , WZ and ZZ production in the POWHEG BOX”, *JHEP* **11** (2011) 078, doi:10.1007/JHEP11(2011)078, arXiv:1107.5051.

- [59] M. Beneke, P. Falgari, S. Klein, and C. Schwinn, “Hadronic top-quark pair production with NNLL threshold resummation”, *Nucl. Phys. B* **855** (2012) 695, doi:10.1016/j.nuclphysb.2011.10.021, arXiv:1109.1536.
- [60] M. Cacciari et al., “Top-pair production at hadron colliders with next-to-next-to-leading logarithmic soft-gluon resummation”, *Phys. Lett. B* **710** (2012) 612, doi:10.1016/j.physletb.2012.03.013, arXiv:1111.5869.
- [61] P. Bärnreuther, M. Czakon, and A. Mitov, “Percent level precision physics at the Tevatron: first genuine NNLO QCD corrections to $q\bar{q} \rightarrow t\bar{t} + X$ ”, *Phys. Rev. Lett.* **109** (2012) 132001, doi:10.1103/PhysRevLett.109.132001, arXiv:1204.5201.
- [62] M. Czakon and A. Mitov, “NNLO corrections to top-pair production at hadron colliders: the all-fermionic scattering channels”, *JHEP* **12** (2012) 054, doi:10.1007/JHEP12(2012)054, arXiv:1207.0236.
- [63] M. Czakon and A. Mitov, “NNLO corrections to top pair production at hadron colliders: the quark-gluon reaction”, *JHEP* **01** (2013) 080, doi:10.1007/JHEP01(2013)080, arXiv:1210.6832.
- [64] M. Czakon, P. Fiedler, and A. Mitov, “Total top-quark pair-production cross section at hadron colliders through $O(\alpha_s^4)$ ”, *Phys. Rev. Lett.* **110** (2013) 252004, doi:10.1103/PhysRevLett.110.252004, arXiv:1303.6254.
- [65] R. Gavin, Y. Li, F. Petriello, and S. Quackenbush, “W physics at the LHC with FEWZ 2.1”, *Comput. Phys. Commun.* **184** (2013) 208, doi:10.1016/j.cpc.2012.09.005, arXiv:1201.5896.
- [66] R. Gavin, Y. Li, F. Petriello, and S. Quackenbush, “FEWZ 2.0: A code for hadronic Z production at next-to-next-to-leading order”, *Comput. Phys. Commun.* **182** (2011) 2388, doi:10.1016/j.cpc.2011.06.008, arXiv:1011.3540.
- [67] GEANT4 Collaboration, “GEANT4—a simulation toolkit”, *Nucl. Instrum. Meth. A* **506** (2003) 250, doi:10.1016/S0168-9002(03)01368-8.
- [68] W. Beenakker, R. Höpker, M. Spira, and P. M. Zerwas, “Squark and gluino production at hadron colliders”, *Nucl. Phys. B* **492** (1997) 51, doi:10.1016/S0550-3213(97)00084-9, arXiv:hep-ph/9610490.
- [69] A. Kulesza and L. Motyka, “Threshold resummation for squark-antisquark and gluino-pair production at the LHC”, *Phys. Rev. Lett.* **102** (2009) 111802, doi:10.1103/PhysRevLett.102.111802, arXiv:0807.2405.
- [70] A. Kulesza and L. Motyka, “Soft gluon resummation for the production of gluino-gluino and squark-antisquark pairs at the LHC”, *Phys. Rev. D* **80** (2009) 095004, doi:10.1103/PhysRevD.80.095004, arXiv:0905.4749.
- [71] W. Beenakker et al., “Soft-gluon resummation for squark and gluino hadroproduction”, *JHEP* **12** (2009) 041, doi:10.1088/1126-6708/2009/12/041, arXiv:0909.4418.
- [72] W. Beenakker et al., “Squark and gluino hadroproduction”, *Int. J. Mod. Phys. A* **26** (2011) 2637, doi:10.1142/S0217751X11053560, arXiv:1105.1110.

- [73] W. Beenakker et al., “NNLL-fast: predictions for coloured supersymmetric particle production at the LHC with threshold and Coulomb resummation”, *JHEP* **12** (2016) 133, doi:10.1007/JHEP12(2016)133, arXiv:1607.07741.
- [74] W. Beenakker et al., “NNLL resummation for squark-antisquark pair production at the LHC”, *JHEP* **01** (2012) 076, doi:10.1007/JHEP01(2012)076, arXiv:1110.2446.
- [75] W. Beenakker et al., “Towards NNLL resummation: hard matching coefficients for squark and gluino hadroproduction”, *JHEP* **10** (2013) 120, doi:10.1007/JHEP10(2013)120, arXiv:1304.6354.
- [76] W. Beenakker et al., “NNLL resummation for squark and gluino production at the LHC”, *JHEP* **12** (2014) 023, doi:10.1007/JHEP12(2014)023, arXiv:1404.3134.
- [77] W. Beenakker et al., “Stop production at hadron colliders”, *Nucl. Phys. B* **515** (1998) 3, doi:10.1016/S0550-3213(98)00014-5, arXiv:hep-ph/9710451.
- [78] W. Beenakker et al., “Supersymmetric top and bottom squark production at hadron colliders”, *JHEP* **08** (2010) 098, doi:10.1007/JHEP08(2010)098, arXiv:1006.4771.
- [79] W. Beenakker et al., “NNLL resummation for stop pair-production at the LHC”, *JHEP* **05** (2016) 153, doi:10.1007/JHEP05(2016)153, arXiv:1601.02954.
- [80] T. Sjöstrand et al., “An Introduction to PYTHIA 8.2”, *Comput. Phys. Commun.* **191** (2015) 159, doi:10.1016/j.cpc.2015.01.024, arXiv:1410.3012.
- [81] S. Abdullin et al., “The fast simulation of the CMS detector at LHC”, *J. Phys. Conf. Ser.* **331** (2011) 032049, doi:10.1088/1742-6596/331/3/032049.
- [82] A. Giammanco, “The fast simulation of the CMS experiment”, *J. Phys. Conf. Ser.* **513** (2014) 022012, doi:10.1088/1742-6596/513/2/022012.
- [83] CMS Collaboration, “Event generator tunes obtained from underlying event and multiparton scattering measurements”, *Eur. Phys. J. C* **76** (2016) 155, doi:10.1140/epjc/s10052-016-3988-x, arXiv:1512.00815.
- [84] CMS Collaboration, “Extraction and validation of a new set of CMS PYTHIA8 tunes from underlying-event measurements”, *Eur. Phys. J. C* **80** (2020) 4, doi:10.1140/epjc/s10052-019-7499-4, arXiv:1903.12179.
- [85] NNPDF Collaboration, “Parton distributions with QED corrections”, *Nucl. Phys. B* **877** (2013) 290, doi:10.1016/j.nuclphysb.2013.10.010, arXiv:1308.0598.
- [86] NNPDF Collaboration, “Parton distributions from high-precision collider data”, *Eur. Phys. J. C* **77** (2017) 663, doi:10.1140/epjc/s10052-017-5199-5, arXiv:1706.00428.
- [87] CMS Collaboration, “Search for supersymmetry in multijet events with missing transverse momentum in proton-proton collisions at 13 TeV”, *Phys. Rev. D* **96** (2017) 032003, doi:10.1103/PhysRevD.96.032003, arXiv:1704.07781.
- [88] CMS Collaboration, “Search for new phenomena with the M_{T2} variable in the all-hadronic final state produced in proton-proton collisions at $\sqrt{s} = 13$ TeV”, *Eur. Phys. J. C* **77** (2017) 710, doi:10.1140/epjc/s10052-017-5267-x, arXiv:1705.04650.

-
- [89] CMS Collaboration, “Search for heavy stable charged particles in pp collisions at $\sqrt{s} = 7$ TeV”, *JHEP* **03** (2011) 024, doi:10.1007/JHEP03(2011)024, arXiv:1101.1645.
- [90] CMS Collaboration, “Search for long-lived charged particles in proton-proton collisions at $\sqrt{s} = 13$ TeV”, *Phys. Rev. D* **94** (2016) 112004, doi:10.1103/PhysRevD.94.112004, arXiv:1609.08382.
- [91] UA1 Collaboration, “Experimental observation of isolated large transverse energy electrons with associated missing energy at $\sqrt{s} = 540$ GeV”, *Phys. Lett. B* **122** (1983) 103, doi:10.1016/0370-2693(83)91177-2.
- [92] G. Kasieczka, B. Nachman, M. D. Schwartz, and D. Shih, “Automating the ABCD method with machine learning”, *Phys. Rev. D* **103** (2021) 035021, doi:10.1103/PhysRevD.103.035021, arXiv:2007.14400.
- [93] CMS Collaboration, “Precision luminosity measurement in proton-proton collisions at $\sqrt{s} = 13$ TeV in 2015 and 2016 at CMS”, *Eur. Phys. J. C* **81** (2021) 800, doi:10.1140/epjc/s10052-021-09538-2, arXiv:2104.01927.
- [94] CMS Collaboration, “CMS luminosity measurement for the 2017 data-taking period at $\sqrt{s} = 13$ TeV”, CMS Physics Analysis Summary CMS-PAS-LUM-17-004, 2018.
- [95] CMS Collaboration, “CMS luminosity measurement for the 2018 data-taking period at $\sqrt{s} = 13$ TeV”, CMS Physics Analysis Summary CMS-PAS-LUM-18-002, 2019.
- [96] A. Giraldi, “Precision luminosity measurement with proton-proton collisions at the CMS experiment in Run 2”, in *Proc. 41st Int. Conf. on High Energy Physics (ICHEP2022)*, p. 638. 2022. arXiv:2208.08214. [PoS(ICHEP2022)638]. doi:10.22323/1.414.0638.
- [97] CMS Collaboration, “Performance of missing transverse momentum reconstruction in proton-proton collisions at $\sqrt{s} = 13$ TeV using the CMS detector”, *JINST* **14** (2019) P07004, doi:10.1088/1748-0221/14/07/P07004, arXiv:1903.06078.
- [98] A. Kalogeropoulos and J. Alwall, “The SysCalc code: A tool to derive theoretical systematic uncertainties”, 2018. arXiv:1801.08401.
- [99] S. Catani, D. de Florian, M. Grazzini, and P. Nason, “Soft gluon resummation for Higgs boson production at hadron colliders”, *JHEP* **07** (2003) 028, doi:10.1088/1126-6708/2003/07/028, arXiv:hep-ph/0306211.
- [100] M. Cacciari et al., “The $t\bar{t}$ cross-section at 1.8 and 1.96 TeV: A study of the systematics due to parton densities and scale dependence”, *JHEP* **04** (2004) 068, doi:10.1088/1126-6708/2004/04/068, arXiv:hep-ph/0303085.
- [101] CMS Collaboration, “Pileup mitigation at CMS in 13 TeV data”, *JINST* **15** (2020) P09018, doi:10.1088/1748-0221/15/09/P09018, arXiv:2003.00503.
- [102] G. Cowan, K. Cranmer, E. Gross, and O. Vitells, “Asymptotic formulae for likelihood-based tests of new physics”, *Eur. Phys. J. C* **71** (2011) 1554, doi:10.1140/epjc/s10052-011-1554-0, arXiv:1007.1727. [Erratum: doi:10.1140/epjc/s10052-013-2501-z].
- [103] T. Junk, “Confidence level computation for combining searches with small statistics”, *Nucl. Instrum. Meth. A* **434** (1999) 435, doi:10.1016/S0168-9002(99)00498-2, arXiv:hep-ex/9902006.





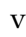
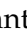




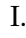







-
- [104] A. L. Read, "Presentation of search results: The CL_s technique", *J. Phys. G* **28** (2002) 2693, doi:10.1088/0954-3899/28/10/313.
- [105] LEP2 SUSY Working Group, ALEPH, DELPHI, L3 and OPAL Collaborations, "Combined LEP chargino results, up to 208 GeV for low Δm ". http://lepsusy.web.cern.ch/lepsusy/www/inoslowdmsummer02/charginolowdm_pub.html, 2002.

A The CMS Collaboration




Yerevan Physics Institute, Yerevan, Armenia

A. Hayrapetyan, A. Tumasyan¹ 

Institut für Hochenergiephysik, Vienna, Austria

W. Adam , J.W. Andrejkovic, T. Bergauer , S. Chatterjee , K. Damanakis , M. Dragicevic , A. Escalante Del Valle , P.S. Hussain , M. Jeitler² , N. Krammer , D. Liko , I. Mikulec , J. Schieck² , R. Schöffbeck , D. Schwarz , M. Sonawane , S. Templ , W. Waltenberger , C.-E. Wulz² 








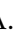



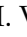


Universiteit Antwerpen, Antwerpen, Belgium

M.R. Darwish³ , T. Janssen , P. Van Mechelen 

Vrije Universiteit Brussel, Brussel, Belgium

E.S. Bols , J. D'Hondt , S. Dansana , A. De Moor , M. Delcourt , H. El Faham , S. Lowette , I. Makarenko , D. Müller , A.R. Sahasransu , S. Tavernier , M. Tytgat⁴ , S. Van Putte , D. Vannerom 

Université Libre de Bruxelles, Bruxelles, Belgium

B. Clerbaux , G. De Lentdecker , L. Favart , D. Hohov , J. Jaramillo , A. Khalilzadeh, K. Lee , M. Mahdavihorrani , A. Malara , S. Paredes , L. Pétré , N. Postiau, L. Thomas , M. Vanden Bemden , C. Vander Velde , P. Vanlaer 






Ghent University, Ghent, Belgium

M. De Coen , D. Dobur , Y. Hong , J. Knolle , L. Lambrecht , G. Mestdach, C. Rendón, A. Samalan, K. Skovpen , N. Van Den Bossche , L. Wezenbeek 




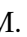










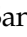



Université Catholique de Louvain, Louvain-la-Neuve, Belgium

A. Benecke , G. Bruno , C. Caputo , C. Delaere , I.S. Donertas , A. Giammanco , K. Jaffel , Sa. Jain , V. Lemaitre, J. Lidrych , P. Mastrapasqua , K. Mondal , T.T. Tran , S. Wertz 

Centro Brasileiro de Pesquisas Físicas, Rio de Janeiro, Brazil

G.A. Alves , E. Coelho , C. Hensel , T. Menezes De Oliveira, A. Moraes , P. Rebello Teles , M. Soeiro

Universidade do Estado do Rio de Janeiro, Rio de Janeiro, Brazil

W.L. Aldá Júnior , M. Alves Gallo Pereira , M. Barroso Ferreira Filho , H. Brandao Malbouisson , W. Carvalho , J. Chinellato⁵, E.M. Da Costa , G.G. Da Silveira⁶ , D. De Jesus Damiao , S. Fonseca De Souza , J. Martins⁷ , C. Mora Herrera , K. Mota Amarilo , L. Mundim , H. Nogima , A. Santoro , A. Sznajder , M. Thiel , A. Vilela Pereira 

Universidade Estadual Paulista, Universidade Federal do ABC, São Paulo, Brazil

C.A. Bernardes⁶ , L. Calligaris , T.R. Fernandez Perez Tomei , E.M. Gregores , P.G. Mercadante , S.F. Novaes , B. Orzari , Sandra S. Padula 

Institute for Nuclear Research and Nuclear Energy, Bulgarian Academy of Sciences, Sofia, Bulgaria

A. Aleksandrov , G. Antchev , R. Hadjiiska , P. Iaydjiev , M. Misheva , M. Shopova , G. Sultanov 





University of Sofia, Sofia, Bulgaria

A. Dimitrov , L. Litov , B. Pavlov , P. Petkov , A. Petrov , E. Shumka 

Instituto De Alta Investigación, Universidad de Tarapacá, Casilla 7 D, Arica, Chile

S. Keshri , S. Thakur 




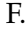


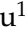
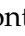




Beihang University, Beijing, China

T. Cheng , Q. Guo, T. Javaid , M. Mittal , L. Yuan 

Department of Physics, Tsinghua University, Beijing, China

G. Bauer^{8,9}, Z. Hu , J. Liu, K. Yi^{8,10} 

Institute of High Energy Physics, Beijing, China

G.M. Chen¹¹ , H.S. Chen¹¹ , M. Chen¹¹ , F. Iemmi , C.H. Jiang, A. Kapoor¹² , H. Liao , Z.-A. Liu¹³ , F. Monti , M.A. Shahzad¹¹, R. Sharma¹⁴ , J.N. Song¹³, J. Tao , C. Wang¹¹, J. Wang , Z. Wang¹¹, H. Zhang 

State Key Laboratory of Nuclear Physics and Technology, Peking University, Beijing, China

A. Agapitos , Y. Ban , A. Levin , C. Li , Q. Li , Y. Mao, S.J. Qian , X. Sun , D. Wang , H. Yang, L. Zhang , C. Zhou 




Sun Yat-Sen University, Guangzhou, China

Z. You 

University of Science and Technology of China, Hefei, China

N. Lu 

Institute of Modern Physics and Key Laboratory of Nuclear Physics and Ion-beam Application (MOE) - Fudan University, Shanghai, China

X. Gao¹⁵ , D. Leggat, H. Okawa , Y. Zhang 





Zhejiang University, Hangzhou, Zhejiang, China

Z. Lin , C. Lu , M. Xiao 





Universidad de Los Andes, Bogota, Colombia

C. Avila , D.A. Barbosa Trujillo, A. Cabrera , C. Florez , J. Fraga , J.A. Reyes Vega

Universidad de Antioquia, Medellin, Colombia

J. Mejia Guisao , F. Ramirez , M. Rodriguez , J.D. Ruiz Alvarez 

University of Split, Faculty of Electrical Engineering, Mechanical Engineering and Naval Architecture, Split, Croatia

D. Giljanovic , N. Godinovic , D. Lelas , A. Sculac 









University of Split, Faculty of Science, Split, Croatia

M. Kovac , T. Sculac 




Institute Rudjer Boskovic, Zagreb, Croatia

P. Bargassa , V. Brigljevic , B.K. Chitroda , D. Ferencek , S. Mishra , A. Starodumov¹⁶ , T. Susa 

University of Cyprus, Nicosia, Cyprus

A. Attikis , K. Christoforou , S. Konstantinou , J. Mousa , C. Nicolaou, F. Ptochos , P.A. Razis , H. Rykaczewski, H. Saka , A. Stepennov 

Charles University, Prague, Czech Republic

M. Finger , M. Finger Jr. , A. Kveton 

Escuela Politecnica Nacional, Quito, Ecuador

E. Ayala 



Universidad San Francisco de Quito, Quito, Ecuador

E. Carrera Jarrin 









Academy of Scientific Research and Technology of the Arab Republic of Egypt, Egyptian Network of High Energy Physics, Cairo, Egypt

S. Elgammal¹⁷, A. Ellithi Kamel¹⁸

Center for High Energy Physics (CHEP-FU), Fayoum University, El-Fayoum, Egypt

A. Lotfy , Y. Mohammed 







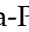
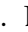







National Institute of Chemical Physics and Biophysics, Tallinn, Estonia

R.K. Dewanjee¹⁹ , K. Ehataht , M. Kadastik, T. Lange , S. Nandan , C. Nielsen , J. Pata , M. Raidal , L. Tani , C. Veelken 

Department of Physics, University of Helsinki, Helsinki, Finland

H. Kirschenmann , K. Osterberg , M. Voutilainen 













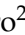


Helsinki Institute of Physics, Helsinki, Finland

S. Bharthuar , E. Brücken , F. Garcia , J. Havukainen , K.T.S. Kallonen , R. Kinnunen, T. Lampén , K. Lassila-Perini , S. Lehti , T. Lindén , M. Lotti, L. Martikainen , M. Myllymäki , M.m. Rantanen , H. Siikonen , E. Tuominen , J. Tuominiemi 




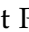










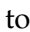















Lappeenranta-Lahti University of Technology, Lappeenranta, Finland

P. Luukka , H. Petrow , T. Tuuva[†]






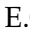








IRFU, CEA, Université Paris-Saclay, Gif-sur-Yvette, France

M. Besancon , F. Couderc , M. Dejardin , D. Denegri, J.L. Faure, F. Ferri , S. Ganjour , P. Gras , G. Hamel de Monchenault , V. Lohezic , J. Malcles , J. Rander, A. Rosowsky , M.Ö. Sahin , A. Savoy-Navarro²⁰ , P. Simkina , M. Titov , M. Tornago 


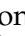
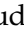






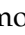

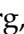



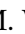


Laboratoire Leprince-Ringuet, CNRS/IN2P3, Ecole Polytechnique, Institut Polytechnique de Paris, Palaiseau, France

C. Baldenegro Barrera , F. Beaudette , A. Buchot Perraguin , P. Busson , A. Cappati , C. Charlot , F. Damas , O. Davignon , A. De Wit , G. Falmagne , B.A. Fontana Santos Alves , S. Ghosh , A. Gilbert , R. Granier de Cassagnac , A. Hakimi , B. Harikrishnan , L. Kalipoliti , G. Liu , J. Motta , M. Nguyen , C. Ochando , L. Portales , R. Salerno , U. Sarkar , J.B. Sauvan , Y. Sirois , A. Tarabini , E. Vernazza , A. Zabi , A. Zghiche 




Université de Strasbourg, CNRS, IPHC UMR 7178, Strasbourg, France

J.-L. Agram²¹ , J. Andrea , D. Apparù , D. Bloch , J.-M. Brom , E.C. Chabert , C. Collard , S. Falke , U. Goerlach , C. Grimault, R. Haeberle , A.-C. Le Bihan , G. Saha , M.A. Sessini , P. Van Hove 




Institut de Physique des 2 Infinis de Lyon (IP2I), Villeurbanne, France

S. Beauceron , B. Blancon , G. Boudoul , N. Chanon , J. Choi , D. Contardo , P. Depasse , C. Dozen²² , H. El Mamouni, J. Fay , S. Gascon , M. Gouzevitch , C. Greenberg, G. Grenier , B. Ille , I.B. Laktineh, M. Lethuillier , L. Mirabito, S. Perries, A. Purohit , M. Vander Donckt , P. Verdier , J. Xiao 

Georgian Technical University, Tbilisi, Georgia

A. Khvedelidze¹⁶ , I. Lomidze , Z. Tsamalaidze¹⁶ 

RWTH Aachen University, I. Physikalisches Institut, Aachen, Germany

V. Botta , L. Feld , K. Klein , M. Lipinski , D. Meuser , A. Pauls , N. Röwert 

G. Anagnostou, P. Assiouras , G. Daskalakis , A. Kyriakis, A. Papadopoulos³¹, A. Stakia 








National and Kapodistrian University of Athens, Athens, Greece

P. Kontaxakis , G. Melachroinos, A. Panagiotou, I. Papavergou , I. Paraskevas , N. Saoulidou , K. Theofilatos , E. Tziaferi , K. Vellidis , I. Zisopoulos 






National Technical University of Athens, Athens, Greece

G. Bakas , T. Chatzistavrou, G. Karapostoli , K. Kousouris , I. Papakrivopoulos , E. Siamarkou, G. Tsiapolitis, A. Zacharopoulou

University of Ioánnina, Ioánnina, Greece

K. Adamidis, I. Bestintzanos, I. Evangelou , C. Foudas, P. Gianneios , C. Kamtsikis, P. Katsoulis, P. Kokkas , P.G. Kosmoglou Kioseoglou , N. Manthos , I. Papadopoulos , J. Strologas 



HUN-REN Wigner Research Centre for Physics, Budapest, Hungary

M. Bartók³² , C. Hajdu , D. Horvath^{33,34} , F. Sikler , V. Veszpremi 

MTA-ELTE Lendület CMS Particle and Nuclear Physics Group, Eötvös Loránd University, Budapest, Hungary

M. Csanád , K. Farkas , M.M.A. Gadallah³⁵ , Á. Kadlecik , P. Major , K. Mandal , G. Pásztor , A.J. Rádl³⁶ , G.I. Veres 




Faculty of Informatics, University of Debrecen, Debrecen, Hungary

P. Raics, B. Ujvari³⁷ , G. Zilizi 









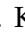
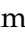





Institute of Nuclear Research ATOMKI, Debrecen, Hungary

G. Bencze, S. Czellar, J. Karancsi³² , J. Molnar, Z. Szillasi

Karoly Robert Campus, MATE Institute of Technology, Gyongyos, Hungary

T. Csorgo³⁶ , F. Nemes³⁶ , T. Novak 









Panjab University, Chandigarh, India

J. Babbar , S. Bansal , S.B. Beri, V. Bhatnagar , G. Chaudhary , S. Chauhan , N. Dhingra³⁸ , A. Kaur , A. Kaur , H. Kaur , M. Kaur , S. Kumar , M. Meena , K. Sandeep , T. Sheokand, J.B. Singh , A. Singla 
















University of Delhi, Delhi, India

A. Ahmed , A. Bhardwaj , A. Chhetri , B.C. Choudhary , A. Kumar , M. Naimuddin , K. Ranjan , S. Saumya 




Saha Institute of Nuclear Physics, HBNI, Kolkata, India

S. Acharya³⁹ , S. Baradia , S. Barman⁴⁰ , S. Bhattacharya , D. Bhowmik, S. Dutta , S. Dutta, B. Gomber³⁹ , P. Palit , B. Sahu³⁹ , S. Sarkar












Indian Institute of Technology Madras, Madras, India

M.M. Ameen , P.K. Behera , S.C. Behera , S. Chatterjee , P. Jana , P. Kalbhor , J.R. Komaragiri⁴¹ , D. Kumar⁴¹ , L. Panwar⁴¹ , R. Pradhan , P.R. Pujahari , N.R. Saha , A. Sharma , A.K. Sikdar , S. Verma 

Tata Institute of Fundamental Research-A, Mumbai, India













T. Aziz, I. Das , S. Dugad, M. Kumar , G.B. Mohanty , P. Suryadevara

Tata Institute of Fundamental Research-B, Mumbai, India

A. Bala , S. Banerjee , R.M. Chatterjee, M. Guchait , Sh. Jain , S. Karmakar , S. Kumar , G. Majumder , K. Mazumdar , S. Mukherjee , S. Parolia , A. Thachayath 

G. Della Ricca^{a,b} 

Kyungpook National University, Daegu, Korea

S. Dogra , J. Hong , C. Huh , B. Kim , D.H. Kim , J. Kim, H. Lee, S.W. Lee ,
C.S. Moon , Y.D. Oh , S.I. Pak , M.S. Ryu , S. Sekmen , Y.C. Yang 

Department of Mathematics and Physics - GWNNU, Gangneung, Korea

M.S. Kim 

Chonnam National University, Institute for Universe and Elementary Particles, Kwangju, Korea

G. Bak , P. Gwak , H. Kim , D.H. Moon 

Hanyang University, Seoul, Korea

E. Asilar , D. Kim , T.J. Kim , J.A. Merlin

Korea University, Seoul, Korea

S. Choi , S. Han, B. Hong , K. Lee, K.S. Lee , S. Lee , J. Park, S.K. Park, J. Yoo 

Kyung Hee University, Department of Physics, Seoul, Korea

J. Goh 


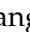




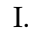

Sejong University, Seoul, Korea

H. S. Kim , Y. Kim, S. Lee


Seoul National University, Seoul, Korea

J. Almond, J.H. Bhyun, J. Choi , W. Jun , J. Kim , J.S. Kim, S. Ko , H. Kwon , H. Lee ,
J. Lee , J. Lee , B.H. Oh , S.B. Oh , H. Seo , U.K. Yang, I. Yoon 

University of Seoul, Seoul, Korea

W. Jang , D.Y. Kang, Y. Kang , S. Kim , B. Ko, J.S.H. Lee , Y. Lee , I.C. Park , Y. Roh,
I.J. Watson , S. Yang 

Yonsei University, Department of Physics, Seoul, Korea

S. Ha , H.D. Yoo 

Sungkyunkwan University, Suwon, Korea

M. Choi , M.R. Kim , H. Lee, Y. Lee , I. Yu 


**College of Engineering and Technology, American University of the Middle East (AUM),
Dasman, Kuwait**

T. Beyrouthy, Y. Maghrbi 

Riga Technical University, Riga, Latvia

K. Dreimanis , A. Gaile , G. Pikurs, A. Potrebko , M. Seidel , V. Veckalns⁵⁷ 

University of Latvia (LU), Riga, Latvia

N.R. Strautnieks 



Vilnius University, Vilnius, Lithuania

M. Ambrozas , A. Juodagalvis , A. Rinkevicius , G. Tamulaitis 





National Centre for Particle Physics, Universiti Malaya, Kuala Lumpur, Malaysia

N. Bin Norjoharuddeen , I. Yusuff⁵⁸ , Z. Zolkapli

Universidad de Sonora (UNISON), Hermosillo, Mexico

J.F. Benitez , A. Castaneda Hernandez , H.A. Encinas Acosta, L.G. Gallegos Maríñez,
M. León Coello , J.A. Murillo Quijada , A. Sehrawat , L. Valencia Palomo 

Centro de Investigacion y de Estudios Avanzados del IPN, Mexico City, Mexico

G. Ayala , H. Castilla-Valdez , E. De La Cruz-Burelo , I. Heredia-De La Cruz⁵⁹ ,
R. Lopez-Fernandez , C.A. Mondragon Herrera, A. Sánchez Hernández 


Universidad Iberoamericana, Mexico City, Mexico

C. Oropeza Barrera , M. Ramírez García 


Benemerita Universidad Autonoma de Puebla, Puebla, Mexico

I. Bautista , I. Pedraza , H.A. Salazar Ibarguen , C. Uribe Estrada 





University of Montenegro, Podgorica, Montenegro

I. Bubanja, N. Raicevic 

University of Canterbury, Christchurch, New Zealand

P.H. Butler 

National Centre for Physics, Quaid-I-Azam University, Islamabad, Pakistan

A. Ahmad , M.I. Asghar, A. Awais , M.I.M. Awan, H.R. Hoorani , W.A. Khan 


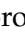




AGH University of Krakow, Faculty of Computer Science, Electronics and Telecommunications, Krakow, Poland

V. Avati, L. Grzanka , M. Malawski 

National Centre for Nuclear Research, Swierk, Poland

H. Bialkowska , M. Bluj , B. Boimska , M. Górski , M. Kazana , M. Szeleper ,
P. Zalewski 
















Institute of Experimental Physics, Faculty of Physics, University of Warsaw, Warsaw, Poland

K. Bunkowski , K. Doroba , A. Kalinowski , M. Konecki , J. Krolikowski ,
A. Muhammad 



Warsaw University of Technology, Warsaw, Poland

K. Pozniak , W. Zabolotny 

Laboratório de Instrumentação e Física Experimental de Partículas, Lisboa, Portugal

M. Araujo , D. Bastos , C. Beirão Da Cruz E Silva , A. Boletti , M. Bozzo ,
G. Da Molin , P. Faccioli , M. Gallinaro , J. Hollar , N. Leonardo , T. Niknejad ,
A. Petrilli , M. Pisano , J. Seixas , J. Varela , J.W. Wulff



























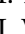
Faculty of Physics, University of Belgrade, Belgrade, Serbia

P. Adzic , P. Milenovic 

VINCA Institute of Nuclear Sciences, University of Belgrade, Belgrade, Serbia

M. Dordevic , J. Milosevic , V. Rekovic

Centro de Investigaciones Energéticas Medioambientales y Tecnológicas (CIEMAT), Madrid, Spain

M. Aguilar-Benitez, J. Alcaraz Maestre , Cristina F. Bedoya , M. Cepeda , M. Cerrada , N. Colino , B. De La Cruz , A. Delgado Peris , D. Fernández Del Val ,
J.P. Fernández Ramos , J. Flix , M.C. Fouz , O. Gonzalez Lopez , S. Goy Lopez ,
J.M. Hernandez , M.I. Josa , J. León Holgado , D. Moran , C. M. Morcillo Perez ,
Á. Navarro Tobar , C. Perez Dengra , A. Pérez-Calero Yzquierdo , J. Puerta Pelayo ,
I. Redondo , D.D. Redondo Ferrero , L. Romero, S. Sánchez Navas , L. Urda Gómez ,
J. Vazquez Escobar , C. Willmott

Universidad Autónoma de Madrid, Madrid, Spain

J.F. de Trocóniz

Universidad de Oviedo, Instituto Universitario de Ciencias y Tecnologías Espaciales de Asturias (ICTEA), Oviedo, Spain

B. Alvarez Gonzalez , J. Cuevas , J. Fernandez Menendez , S. Folgueras , I. Gonzalez Caballero , J.R. González Fernández , E. Palencia Cortezon , C. Ramón Álvarez , V. Rodríguez Bouza , A. Soto Rodríguez , A. Trapote , C. Vico Villalba , P. Vischia

Instituto de Física de Cantabria (IFCA), CSIC-Universidad de Cantabria, Santander, Spain

S. Bhowmik , S. Blanco Fernández , J.A. Brochero Cifuentes , I.J. Cabrillo , A. Calderon , J. Duarte Campderros , M. Fernandez , C. Fernandez Madrazo , G. Gomez , C. Lasaos García , C. Martinez Rivero , P. Martinez Ruiz del Arbol , F. Matorras , P. Matorras Cuevas , E. Navarrete Ramos , J. Piedra Gomez , L. Scodellaro , I. Vila , J.M. Vizan Garcia

University of Colombo, Colombo, Sri Lanka

M.K. Jayananda , B. Kailasapathy⁶⁰ , D.U.J. Sonnadara , D.D.C. Wickramarathna

University of Ruhuna, Department of Physics, Matara, Sri Lanka

W.G.D. Dharmaratna , K. Liyanage , N. Perera , N. Wickramage

CERN, European Organization for Nuclear Research, Geneva, Switzerland

D. Abbaneo , C. Amendola , E. Auffray , G. Auzinger , J. Baechler, D. Barney , A. Bermúdez Martínez , M. Bianco , B. Bilin , A.A. Bin Anuar , A. Bocci , E. Brondolin , C. Caillol , T. Camporesi , G. Cerminara , N. Chernyavskaya , D. d'Enterria , A. Dabrowski , A. David , A. De Roeck , M.M. Defranchis , M. Deile , M. Dobson , F. Fallavollita⁶¹, L. Forthomme , G. Franzoni , W. Funk , S. Giani, D. Gigi, K. Gill , F. Glege , L. Gouskos , M. Haranko , J. Hegeman , B. Huber, V. Innocente , T. James , P. Janot , S. Laurila , P. Lecoq , E. Leutgeb , C. Lourenço , B. Maier , L. Malgeri , M. Mannelli , A.C. Marini , M. Matthewman, F. Meijers , S. Mersi , E. Meschi , V. Milosevic , F. Moortgat , M. Mulders , S. Orfanelli, F. Pantaleo , G. Petrucciani , A. Pfeiffer , M. Pierini , D. Piparo , H. Qu , D. Rabady , G. Reales Gutiérrez, M. Rovere , H. Sakulin , S. Scarfi , C. Schwick, M. Selvaggi , A. Sharma , K. Shchelina , P. Silva , P. Sphicas⁶² , A.G. Stahl Leitner , A. Steen , S. Summers , D. Treille , P. Tropea , A. Tsirou, D. Walter , J. Wanczyk⁶³ , K.A. Wozniak⁶⁴ , S. Wuchterl , P. Zehetner , P. Zejdl , W.D. Zeuner

Paul Scherrer Institut, Villigen, Switzerland



















T. Bevilacqua⁶⁵ , L. Caminada⁶⁵ , A. Ebrahimi , W. Erdmann , R. Horisberger , Q. Ingram , H.C. Kaestli , D. Kotlinski , C. Lange , M. Missiroli⁶⁵ , L. Noehte⁶⁵ , T. Rohe

ETH Zurich - Institute for Particle Physics and Astrophysics (IPA), Zurich, Switzerland

T.K. Aarrestad , K. Androsov⁶³ , M. Backhaus , A. Calandri , C. Cazzaniga , K. Datta , A. De Cosa , G. Dissertori , M. Dittmar, M. Donegà , F. Eble , M. Galli , K. Gedia , F. Glessgen , C. Grab , D. Hits , W. Lustermann , A.-M. Lyon , R.A. Manzoni , M. Marchegiani , L. Marchese , C. Martin Perez , A. Mascellani⁶³ , E. Nessi-Tedaldi , F. Pauss , V. Perovic , S. Pigazzini , M.G. Ratti , M. Reichmann , C. Reissel , T. Reitenspiess , B. Ristic , F. Riti , D. Ruini, D.A. Sanz Becerra , R. Seidita , J. Steggemann⁶³ , D. Valsecchi , R. Wallny

Universität Zürich, Zurich, Switzerland










C. Amsler⁶⁶ , P. Bäertschi , C. Botta , D. Brzhechko, M.F. Canelli , K. Cormier

R. Del Burgo, J.K. Heikkilä , M. Huwiler , W. Jin , A. Jofrehei , B. Kilminster , S. Leontsinis , S.P. Liechti , A. Macchiolo , P. Meiring , V.M. Mikuni , U. Molinatti , I. Neutelings , A. Reimers , P. Robmann, S. Sanchez Cruz , K. Schweiger , M. Senger , Y. Takahashi , R. Tramontano 


National Central University, Chung-Li, Taiwan

C. Adloff⁶⁷, C.M. Kuo, W. Lin, P.K. Rout , P.C. Tiwari⁴¹ , S.S. Yu 












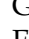





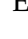

National Taiwan University (NTU), Taipei, Taiwan

L. Ceard, Y. Chao , K.F. Chen , P.s. Chen, Z.g. Chen, W.-S. Hou , T.h. Hsu, Y.w. Kao, R. Khurana, G. Kole , Y.y. Li , R.-S. Lu , E. Paganis , A. Psallidas, X.f. Su, J. Thomas-Wilsker , L.s. Tsai, H.y. Wu, E. Yazgan 


High Energy Physics Research Unit, Department of Physics, Faculty of Science, Chulalongkorn University, Bangkok, Thailand

C. Asawatangtrakuldee , N. Srimanobhas , V. Wachirapusanand 

Çukurova University, Physics Department, Science and Art Faculty, Adana, Turkey

D. Agyel , F. Boran , Z.S. Demiroglu , F. Dolek , I. Dumanoglu⁶⁸ , E. Eskut , Y. Guler⁶⁹ , E. Gurpinar Guler⁶⁹ , C. Isik , O. Kara, A. Kayis Topaksu , U. Kiminsu , G. Onengut , K. Ozdemir⁷⁰ , A. Polatoz , B. Tali⁷¹ , U.G. Tok , S. Turkcapar , E. Uslan , I.S. Zorbakir 

Middle East Technical University, Physics Department, Ankara, Turkey

M. Yalvac⁷² 




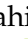



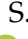
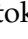


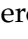

Bogazici University, Istanbul, Turkey

B. Akgun , I.O. Atakisi , E. Gülmez , M. Kaya⁷³ , O. Kaya⁷⁴ , S. Tekten⁷⁵ 

Istanbul Technical University, Istanbul, Turkey

A. Cakir , K. Cankocak^{68,76} , Y. Komurcu , S. Sen⁷⁷ 

Istanbul University, Istanbul, Turkey

O. Aydilek , S. Cerci⁷¹ , V. Epshteyn , B. Hacisahinoglu , I. Hos⁷⁸ , B. Isildak⁷⁹ , B. Kaynak , S. Ozkorucuklu , O. Potok , H. Sert , C. Simsek , D. Sunar Cerci⁷¹ , C. Zorbilmez 







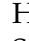

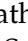
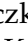




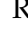
Institute for Scintillation Materials of National Academy of Science of Ukraine, Kharkiv, Ukraine

A. Boyaryntsev , B. Grynyov 





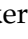




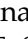







National Science Centre, Kharkiv Institute of Physics and Technology, Kharkiv, Ukraine

L. Levchuk 









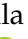




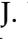

















University of Bristol, Bristol, United Kingdom

D. Anthony , J.J. Brooke , A. Bundock , F. Bury , E. Clement , D. Cussans , H. Flacher , M. Glowacki, J. Goldstein , H.F. Heath , L. Kreczko , B. Krikler , S. Paramesvaran , S. Seif El Nasr-Storey, V.J. Smith , N. Stylianou⁸⁰ , K. Walkingshaw Pass, R. White 




Rutherford Appleton Laboratory, Didcot, United Kingdom

A.H. Ball, K.W. Bell , A. Belyaev⁸¹ , C. Brew , R.M. Brown , D.J.A. Cockerill , C. Cooke , K.V. Ellis, K. Harder , S. Harper , M.-L. Holmberg⁸² , J. Linacre , K. Manolopoulos, D.M. Newbold , E. Olaiya, D. Petyt , T. Reis , G. Salvi , T. Schuh, C.H. Shepherd-Themistocleous , I.R. Tomalin , T. Williams 





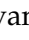
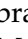







Imperial College, London, United Kingdom

R. Bainbridge , P. Bloch , C.E. Brown , O. Buchmuller, V. Cacchio, C.A. Carrillo Montoya , G.S. Chahal⁸³ , D. Colling , J.S. Dancu, P. Dauncey , G. Davies , J. Davies, M. Della Negra , S. Fayer, G. Fedi , G. Hall , M.H. Hassanshahi , A. Howard, G. Iles , M. Knight , J. Langford , L. Lyons , A.-M. Magnan , S. Malik, A. Martelli , M. Mieskolainen , J. Nash⁸⁴ , M. Pesaresi, B.C. Radburn-Smith , A. Richards, A. Rose , C. Seez , R. Shukla , A. Tapper , K. Uchida , G.P. Uttley , L.H. Vage, T. Virdee³¹ , M. Vojinovic , N. Wardle , D. Winterbottom 

Brunel University, Uxbridge, United Kingdom

K. Coldham, J.E. Cole , A. Khan, P. Kyberd , I.D. Reid 

Baylor University, Waco, Texas, USA

S. Abdullin , A. Brinkerhoff , B. Caraway , J. Dittmann , K. Hatakeyama , J. Hiltbrand , A.R. Kanuganti , B. McMaster , M. Saunders , S. Sawant , C. Sutantawibul , M. Toms⁸⁵ , J. Wilson 



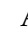



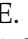


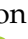

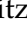
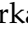
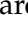


Catholic University of America, Washington, DC, USA

R. Bartek , A. Dominguez , C. Huerta Escamilla, A.E. Simsek , R. Uniyal , A.M. Vargas Hernandez 













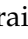

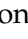
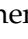

The University of Alabama, Tuscaloosa, Alabama, USA

R. Chudasama , S.I. Cooper , S.V. Gleyzer , C.U. Perez , P. Rumerio⁸⁶ , E. Usai , C. West , R. Yi 



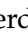







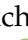
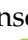
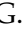

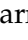

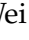

Boston University, Boston, Massachusetts, USA

A. Akpinar , A. Albert , D. Arcaro , C. Cosby , Z. Demiragli , C. Erice , E. Fontanesi , D. Gastler , S. Jeon , J. Rohlf , K. Salyer , D. Sperka , D. Spitzbart , I. Suarez , A. Tsatsos , S. Yuan 

Brown University, Providence, Rhode Island, USA

G. Benelli , X. Coubez²⁶, D. Cutts , M. Hadley , U. Heintz , J.M. Hogan⁸⁷ , T. Kwon , G. Landsberg , K.T. Lau , D. Li , J. Luo , S. Mondal , M. Narain[†] , N. Pervan , S. Sagir⁸⁸ , F. Simpson , M. Stamenkovic , W.Y. Wong, X. Yan , W. Zhang

University of California, Davis, Davis, California, USA

S. Abbott , J. Bonilla , C. Brainerd , R. Breedon , M. Calderon De La Barca Sanchez , M. Chertok , M. Citron , J. Conway , P.T. Cox , R. Erbacher , F. Jensen , O. Kukral , G. Mocellin , M. Mulhearn , D. Pellett , W. Wei , Y. Yao , F. Zhang 










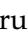








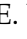


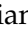
University of California, Los Angeles, California, USA

M. Bachtis , R. Cousins , A. Datta , J. Hauser , M. Ignatenko , M.A. Iqbal , T. Lam , E. Manca , D. Saltzberg , V. Valuev 

















University of California, Riverside, Riverside, California, USA

R. Clare , J.W. Gary , M. Gordon, G. Hanson , W. Si , S. Wimpenny[†] 


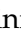









University of California, San Diego, La Jolla, California, USA

J.G. Branson , S. Cittolin , S. Cooperstein , D. Diaz , J. Duarte , L. Giannini , J. Guiang , R. Kansal , V. Krutlyov , R. Lee , J. Letts , M. Masciovecchio , F. Mokhtar , M. Pieri , M. Quinnan , B.V. Sathia Narayanan , V. Sharma , M. Tadel , E. Vourliotis , F. Würthwein , Y. Xiang , A. Yagil 













University of California, Santa Barbara - Department of Physics, Santa Barbara, California, USA

mov , C.E. Gerber , D.J. Hofman , J.h. Lee , D. S. Lemos , A.H. Merrit , C. Mills , S. Nanda , G. Oh , B. Ozek , D. Pilipovic , T. Roy , S. Rudrabhatla , M.B. Tonjes , N. Varelas , X. Wang , Z. Ye , J. Yoo 

























The University of Iowa, Iowa City, Iowa, USA

M. Alhousseini , D. Blend, K. Dilsiz⁹¹ , L. Emediato , G. Karaman , O.K. Köseyan , J.-P. Merlo, A. Mestvirishvili⁹² , J. Nachtman , O. Neogi, H. Ogul⁹³ , Y. Onel , A. Penzo , C. Snyder, E. Tiras⁹⁴ 









Johns Hopkins University, Baltimore, Maryland, USA

B. Blumenfeld , L. Corcodilos , J. Davis , A.V. Gritsan , L. Kang , S. Kyriacou , P. Maksimovic , M. Roguljic , J. Roskes , S. Sekhar , M. Swartz , T.Á. Vámi 

The University of Kansas, Lawrence, Kansas, USA

A. Abreu , L.F. Alcerro Alcerro , J. Anguiano , P. Baringer , A. Bean , Z. Flowers , D. Grove , J. King , G. Krintiras , M. Lazarovits , C. Le Mahieu , C. Lindsey, J. Marquez , N. Minafra , M. Murray , M. Nickel , M. Pitt , S. Popescu⁹⁵ , C. Rogan , C. Royon , R. Salvatico , S. Sanders , C. Smith , Q. Wang , G. Wilson 

















Kansas State University, Manhattan, Kansas, USA

B. Allmond , A. Ivanov , K. Kaadze , A. Kalogeropoulos , D. Kim, Y. Maravin , K. Nam, J. Natoli , D. Roy , G. Sorrentino 

























Lawrence Livermore National Laboratory, Livermore, California, USA

F. Rebassoo , D. Wright 















University of Maryland, College Park, Maryland, USA

A. Baden , A. Belloni , A. Bethani , Y.M. Chen , S.C. Eno , N.J. Hadley , S. Jabeen , R.G. Kellogg , T. Koeth , Y. Lai , S. Lascio , A.C. Mignerey , S. Nabili , C. Palmer , C. Papageorgakis , M.M. Paranjpe, L. Wang 

Massachusetts Institute of Technology, Cambridge, Massachusetts, USA

J. Bendavid , W. Busza , I.A. Cali , Y. Chen , M. D'Alfonso , J. Eysermans , C. Freer , G. Gomez-Ceballos , M. Goncharov, P. Harris, D. Hoang, D. Kovalskyi , J. Krupa , L. Lavezzo , Y.-J. Lee , K. Long , C. Mironov , C. Paus , D. Rankin , C. Roland , G. Roland , S. Rothman , Z. Shi , G.S.F. Stephans , J. Wang, Z. Wang , B. Wyslouch , T. J. Yang 

University of Minnesota, Minneapolis, Minnesota, USA

B. Crossman , B.M. Joshi , C. Kapsiak , M. Krohn , D. Mahon , J. Mans , B. Marzocchi , S. Pandey , M. Revering , R. Rusack , R. Saradhy , N. Schroeder , N. Strobbe , M.A. Wadud 

University of Mississippi, Oxford, Mississippi, USA

L.M. Cremaldi 

















University of Nebraska-Lincoln, Lincoln, Nebraska, USA

K. Bloom , M. Bryson, D.R. Claes , C. Fangmeier , F. Golf , G. Haza , J. Hossain , C. Joo , I. Kravchenko , I. Reed , J.E. Siado , W. Tabb , A. Vagnerini , A. Wightman , F. Yan , D. Yu , A.G. Zecchinelli 

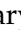









State University of New York at Buffalo, Buffalo, New York, USA

G. Agarwal , H. Bandyopadhyay , L. Hay , I. Iashvili , A. Kharchilava , M. Morris , D. Nguyen , S. Rappoccio , H. Rejeb Sfar, A. Williams 

















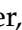









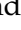





Northeastern University, Boston, Massachusetts, USA

E. Barberis , Y. Haddad , Y. Han , A. Krishna , J. Li , M. Lu , G. Madigan , R. Mccarthy , D.M. Morse , V. Nguyen , T. Orimoto , A. Parker , L. Skinnari , A. Tishelman-Charny , B. Wang , D. Wood 








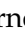

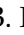

Northwestern University, Evanston, Illinois, USA

S. Bhattacharya , J. Bueghly , Z. Chen , K.A. Hahn , Y. Liu , Y. Miao , D.G. Monk , M.H. Schmitt , A. Taliercio , M. Velasco 









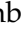

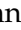




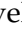



University of Notre Dame, Notre Dame, Indiana, USA

R. Band , R. Bucci , S. Castells , M. Cremonesi , A. Das , R. Goldouzian , M. Hildreth , K.W. Ho , K. Hurtado Anampa , T. Ivanov , C. Jessop , K. Lannon , J. Lawrence , N. Loukas , L. Lutton , J. Mariano , N. Marinelli , I. Mcalister , T. McCauley , C. Mcgrady , C. Moore , Y. Musienko¹⁶ , H. Nelson , M. Osherson , A. Piccinelli , R. Ruchti , A. Townsend , Y. Wan , M. Wayne , H. Yockey , M. Zarucki , L. Zygala 

The Ohio State University, Columbus, Ohio, USA

A. Basnet , B. Bylsma , M. Carrigan , L.S. Durkin , C. Hill , M. Joyce , A. Lesauvage , M. Nunez Ornelas , K. Wei , B.L. Winer , B. R. Yates 















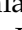

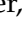
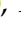


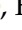


Princeton University, Princeton, New Jersey, USA

F.M. Addesa , H. Bouchamaoui , P. Das , G. Dezoort , P. Elmer , A. Frankenthal , B. Greenberg , N. Haubrich , S. Higginbotham , G. Kopp , S. Kwan , D. Lange , A. Loeliger , D. Marlow , I. Ojalvo , J. Olsen , A. Shevelev , D. Stickland , C. Tully 




University of Puerto Rico, Mayaguez, Puerto Rico, USA

S. Malik 














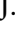
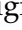
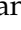
Purdue University, West Lafayette, Indiana, USA

A.S. Bakshi , V.E. Barnes , S. Chandra , R. Chawla , S. Das , A. Gu , L. Gutay , M. Jones , A.W. Jung , D. Kondratyev , A.M. Koshy , M. Liu , G. Negro , N. Neumeister , G. Paspalaki , S. Piperov , V. Scheurer , J.F. Schulte , M. Stojanovic , J. Thieman , A. K. Viridi , F. Wang , W. Xie 


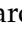
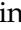


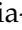


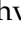
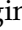


Purdue University Northwest, Hammond, Indiana, USA

J. Dolen , N. Parashar , A. Pathak 

Rice University, Houston, Texas, USA

D. Acosta , A. Baty , T. Carnahan , K.M. Ecklund , P.J. Fernández Manteca , S. Freed , P. Gardner , F.J.M. Geurts , A. Kumar , W. Li , O. Miguel Colin , B.P. Padley , R. Redjimi , J. Rotter , E. Yigitbasi , Y. Zhang 

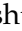


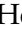



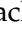


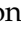
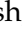

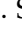





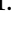

University of Rochester, Rochester, New York, USA

A. Bodek , P. de Barbaro , R. Demina , J.L. Dulemba , C. Fallon , A. Garcia-Bellido , O. Hindrichs , A. Khukhunaishvili , P. Parygin⁸⁵ , E. Popova⁸⁵ , R. Taus , G.P. Van Onsem 









The Rockefeller University, New York, New York, USA

K. Goulios 















Rutgers, The State University of New Jersey, Piscataway, New Jersey, USA

B. Chiarito , J.P. Chou , Y. Gershtein , E. Halkiadakis , A. Hart , M. Heindl , D. Jaroslowski , O. Karacheban²⁹ , I. Laflotte , A. Lath , R. Montalvo , K. Nash , H. Routray , S. Salur , S. Schnetzer , S. Somalwar , R. Stone , S.A. Thayil , S. Thomas , J. Vora , H. Wang 



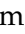








University of Tennessee, Knoxville, Tennessee, USA

H. Acharya, D. Ally , A.G. Delannoy , S. Fiorendi , T. Holmes , N. Karunarathna , L. Lee , E. Nibigira , S. Spanier 

Texas A&M University, College Station, Texas, USA

D. Aebi , M. Ahmad , O. Bouhali⁹⁶ , M. Dalchenko , R. Eusebi , J. Gilmore , T. Huang , T. Kamon⁹⁷ , H. Kim , S. Luo , S. Malhotra, R. Mueller , D. Overton , D. Rathjens , A. Safonov 









Texas Tech University, Lubbock, Texas, USA

N. Akchurin , J. Damgov , V. Hegde , A. Hussain , Y. Kazhykarim, K. Lamichhane , S.W. Lee , A. Mankel , T. Mengke, S. Muthumuni , T. Peltola , I. Volobouev , A. Whitbeck 

Vanderbilt University, Nashville, Tennessee, USA

E. Appelt , S. Greene, A. Gurrola , W. Johns , R. Kunnawalkam Elayavalli , A. Melo , F. Romeo , P. Sheldon , S. Tuo , J. Velkovska , J. Viinikainen 



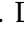
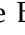
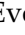

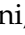
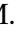

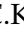

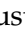









University of Virginia, Charlottesville, Virginia, USA

B. Cardwell , B. Cox , J. Hakala , R. Hirosky , A. Ledovskoy , A. Li , C. Neu , C.E. Perez Lara 

Wayne State University, Detroit, Michigan, USA

P.E. Karchin 

University of Wisconsin - Madison, Madison, Wisconsin, USA

A. Aravind, S. Banerjee , K. Black , T. Bose , S. Dasu , I. De Bruyn , P. Everaerts , C. Galloni, H. He , M. Herndon , A. Herve , C.K. Koraka , A. Lanaro, R. Loveless , J. Madhusudanan Sreekala , A. Mallampalli , A. Mohammadi , S. Mondal, G. Parida , D. Pinna, A. Savin, V. Shang , V. Sharma , W.H. Smith , D. Teague, H.F. Tsoi , W. Vetens , A. Warden 

Authors affiliated with an institute or an international laboratory covered by a cooperation agreement with CERN

S. Afanasiev , V. Andreev , Yu. Andreev , T. Aushev , M. Azarkin , I. Azhgirey , A. Babaev , A. Belyaev , V. Blinov⁹⁸, E. Boos , V. Borshch , D. Budkouski , V. Bunichev , M. Chadeeva⁹⁸ , V. Chekhovsky, M. Danilov⁹⁸ , A. Dermenev , T. Dimova⁹⁸ , D. Druzhkin⁹⁹ , M. Dubinin⁸⁹ , L. Dudko , A. Ershov , G. Gavrilo , V. Gavrilo , S. Gninenko , V. Golovtsov , N. Golubev , I. Golutvin , I. Gorbunov , A. Gribushin , Y. Ivanov , V. Kachanov , L. Kardapoltsev⁹⁸ , V. Karjavine , A. Karneyeu , V. Kim⁹⁸ , M. Kirakosyan, D. Kirpichnikov , M. Kirsanov , V. Klyukhin , O. Kodolova¹⁰⁰ , D. Konstantinov , V. Korenkov , A. Kozyrev⁹⁸ , N. Krasnikov , A. Lanev , P. Levchenko¹⁰¹ , N. Lychkovskaya , V. Makarenko , A. Malakhov , V. Matveev⁹⁸ , V. Murzin , A. Nikitenko^{102,100} , S. Obraztsov , V. Oreshkin , V. Palichik , V. Perelygin , M. Perfilov, S. Petrushanko , S. Polikarpov⁹⁸ , V. Popov, O. Radchenko⁹⁸ , R. Ryutin, M. Savina , V. Savrin , V. Shalaev , S. Shmatov , S. Shulha , Y. Skovpen⁹⁸ , S. Slabospitskii , V. Smirnov , D. Sosnov , V. Sulimov , E. Tcherniaev , A. Terkulov , O. Teryaev , I. Tlisova , A. Toropin , L. Uvarov , A. Uzunian , A. Volkov, A. Vorobyev[†], N. Voytishin , B.S. Yuldashev¹⁰³, A. Zarubin , I. Zhizhin , A. Zhokin 

†: Deceased

¹Also at Yerevan State University, Yerevan, Armenia

-
- ²Also at TU Wien, Vienna, Austria
- ³Also at Institute of Basic and Applied Sciences, Faculty of Engineering, Arab Academy for Science, Technology and Maritime Transport, Alexandria, Egypt
- ⁴Also at Ghent University, Ghent, Belgium
- ⁵Also at Universidade Estadual de Campinas, Campinas, Brazil
- ⁶Also at Federal University of Rio Grande do Sul, Porto Alegre, Brazil
- ⁷Also at UFMS, Nova Andradina, Brazil
- ⁸Also at Nanjing Normal University, Nanjing, China
- ⁹Now at Henan Normal University, Xinxiang, China
- ¹⁰Now at The University of Iowa, Iowa City, Iowa, USA
- ¹¹Also at University of Chinese Academy of Sciences, Beijing, China
- ¹²Also at China Center of Advanced Science and Technology, Beijing, China
- ¹³Also at University of Chinese Academy of Sciences, Beijing, China
- ¹⁴Also at China Spallation Neutron Source, Guangdong, China
- ¹⁵Also at Université Libre de Bruxelles, Bruxelles, Belgium
- ¹⁶Also at an institute or an international laboratory covered by a cooperation agreement with CERN
- ¹⁷Now at British University in Egypt, Cairo, Egypt
- ¹⁸Now at Cairo University, Cairo, Egypt
- ¹⁹Also at Birla Institute of Technology, Mesra, Mesra, India
- ²⁰Also at Purdue University, West Lafayette, Indiana, USA
- ²¹Also at Université de Haute Alsace, Mulhouse, France
- ²²Also at Department of Physics, Tsinghua University, Beijing, China
- ²³Also at The University of the State of Amazonas, Manaus, Brazil
- ²⁴Also at Erzincan Binali Yildirim University, Erzincan, Turkey
- ²⁵Also at University of Hamburg, Hamburg, Germany
- ²⁶Also at RWTH Aachen University, III. Physikalisches Institut A, Aachen, Germany
- ²⁷Also at Isfahan University of Technology, Isfahan, Iran
- ²⁸Also at Bergische University Wuppertal (BUW), Wuppertal, Germany
- ²⁹Also at Brandenburg University of Technology, Cottbus, Germany
- ³⁰Also at Forschungszentrum Jülich, Juelich, Germany
- ³¹Also at CERN, European Organization for Nuclear Research, Geneva, Switzerland
- ³²Also at Institute of Physics, University of Debrecen, Debrecen, Hungary
- ³³Also at Institute of Nuclear Research ATOMKI, Debrecen, Hungary
- ³⁴Now at Universitatea Babeş-Bolyai - Facultatea de Fizica, Cluj-Napoca, Romania
- ³⁵Also at Physics Department, Faculty of Science, Assiut University, Assiut, Egypt
- ³⁶Also at HUN-REN Wigner Research Centre for Physics, Budapest, Hungary
- ³⁷Also at Faculty of Informatics, University of Debrecen, Debrecen, Hungary
- ³⁸Also at Punjab Agricultural University, Ludhiana, India
- ³⁹Also at University of Hyderabad, Hyderabad, India
- ⁴⁰Also at University of Visva-Bharati, Santiniketan, India
- ⁴¹Also at Indian Institute of Science (IISc), Bangalore, India
- ⁴²Also at IIT Bhubaneswar, Bhubaneswar, India
- ⁴³Also at Institute of Physics, Bhubaneswar, India
- ⁴⁴Also at Deutsches Elektronen-Synchrotron, Hamburg, Germany
- ⁴⁵Also at Department of Physics, Isfahan University of Technology, Isfahan, Iran
- ⁴⁶Also at Sharif University of Technology, Tehran, Iran
- ⁴⁷Also at Department of Physics, University of Science and Technology of Mazandaran, Behshahr, Iran

- ⁴⁸Also at Helwan University, Cairo, Egypt
- ⁴⁹Also at Italian National Agency for New Technologies, Energy and Sustainable Economic Development, Bologna, Italy
- ⁵⁰Also at Centro Siciliano di Fisica Nucleare e di Struttura Della Materia, Catania, Italy
- ⁵¹Also at Università degli Studi Guglielmo Marconi, Roma, Italy
- ⁵²Also at Scuola Superiore Meridionale, Università di Napoli 'Federico II', Napoli, Italy
- ⁵³Also at Fermi National Accelerator Laboratory, Batavia, Illinois, USA
- ⁵⁴Also at Università di Napoli 'Federico II', Napoli, Italy
- ⁵⁵Also at Ain Shams University, Cairo, Egypt
- ⁵⁶Also at Consiglio Nazionale delle Ricerche - Istituto Officina dei Materiali, Perugia, Italy
- ⁵⁷Also at Riga Technical University, Riga, Latvia
- ⁵⁸Also at Department of Applied Physics, Faculty of Science and Technology, Universiti Kebangsaan Malaysia, Bangi, Malaysia
- ⁵⁹Also at Consejo Nacional de Ciencia y Tecnología, Mexico City, Mexico
- ⁶⁰Also at Trincomalee Campus, Eastern University, Sri Lanka, Nilaveli, Sri Lanka
- ⁶¹Also at INFN Sezione di Pavia, Università di Pavia, Pavia, Italy
- ⁶²Also at National and Kapodistrian University of Athens, Athens, Greece
- ⁶³Also at Ecole Polytechnique Fédérale Lausanne, Lausanne, Switzerland
- ⁶⁴Also at University of Vienna Faculty of Computer Science, Vienna, Austria
- ⁶⁵Also at Universität Zürich, Zurich, Switzerland
- ⁶⁶Also at Stefan Meyer Institute for Subatomic Physics, Vienna, Austria
- ⁶⁷Also at Laboratoire d'Annecy-le-Vieux de Physique des Particules, IN2P3-CNRS, Annecy-le-Vieux, France
- ⁶⁸Also at Near East University, Research Center of Experimental Health Science, Mersin, Turkey
- ⁶⁹Also at Konya Technical University, Konya, Turkey
- ⁷⁰Also at Izmir Bakircay University, Izmir, Turkey
- ⁷¹Also at Adiyaman University, Adiyaman, Turkey
- ⁷²Also at Bozok Universitetesi Rektörlüğü, Yozgat, Turkey
- ⁷³Also at Marmara University, Istanbul, Turkey
- ⁷⁴Also at Milli Savunma University, Istanbul, Turkey
- ⁷⁵Also at Kafkas University, Kars, Turkey
- ⁷⁶Now at Istanbul Okan University, Istanbul, Turkey
- ⁷⁷Also at Hacettepe University, Ankara, Turkey
- ⁷⁸Also at Istanbul University - Cerrahpasa, Faculty of Engineering, Istanbul, Turkey
- ⁷⁹Also at Yildiz Technical University, Istanbul, Turkey
- ⁸⁰Also at Vrije Universiteit Brussel, Brussel, Belgium
- ⁸¹Also at School of Physics and Astronomy, University of Southampton, Southampton, United Kingdom
- ⁸²Also at University of Bristol, Bristol, United Kingdom
- ⁸³Also at IPPP Durham University, Durham, United Kingdom
- ⁸⁴Also at Monash University, Faculty of Science, Clayton, Australia
- ⁸⁵Now at an institute or an international laboratory covered by a cooperation agreement with CERN
- ⁸⁶Also at Università di Torino, Torino, Italy
- ⁸⁷Also at Bethel University, St. Paul, Minnesota, USA
- ⁸⁸Also at Karamanoğlu Mehmetbey University, Karaman, Turkey
- ⁸⁹Also at California Institute of Technology, Pasadena, California, USA
- ⁹⁰Also at United States Naval Academy, Annapolis, Maryland, USA

⁹¹Also at Bingol University, Bingol, Turkey

⁹²Also at Georgian Technical University, Tbilisi, Georgia

⁹³Also at Sinop University, Sinop, Turkey

⁹⁴Also at Erciyes University, Kayseri, Turkey

⁹⁵Also at Horia Hulubei National Institute of Physics and Nuclear Engineering (IFIN-HH), Bucharest, Romania

⁹⁶Also at Texas A&M University at Qatar, Doha, Qatar

⁹⁷Also at Kyungpook National University, Daegu, Korea

⁹⁸Also at another institute or international laboratory covered by a cooperation agreement with CERN

⁹⁹Also at Universiteit Antwerpen, Antwerpen, Belgium

¹⁰⁰Also at Yerevan Physics Institute, Yerevan, Armenia

¹⁰¹Also at Northeastern University, Boston, Massachusetts, USA

¹⁰²Also at Imperial College, London, United Kingdom

¹⁰³Also at Institute of Nuclear Physics of the Uzbekistan Academy of Sciences, Tashkent, Uzbekistan